EEP20/11

IMPACT OF ICE ON SWEDISH OFFSHORE LIGHTHOUSES

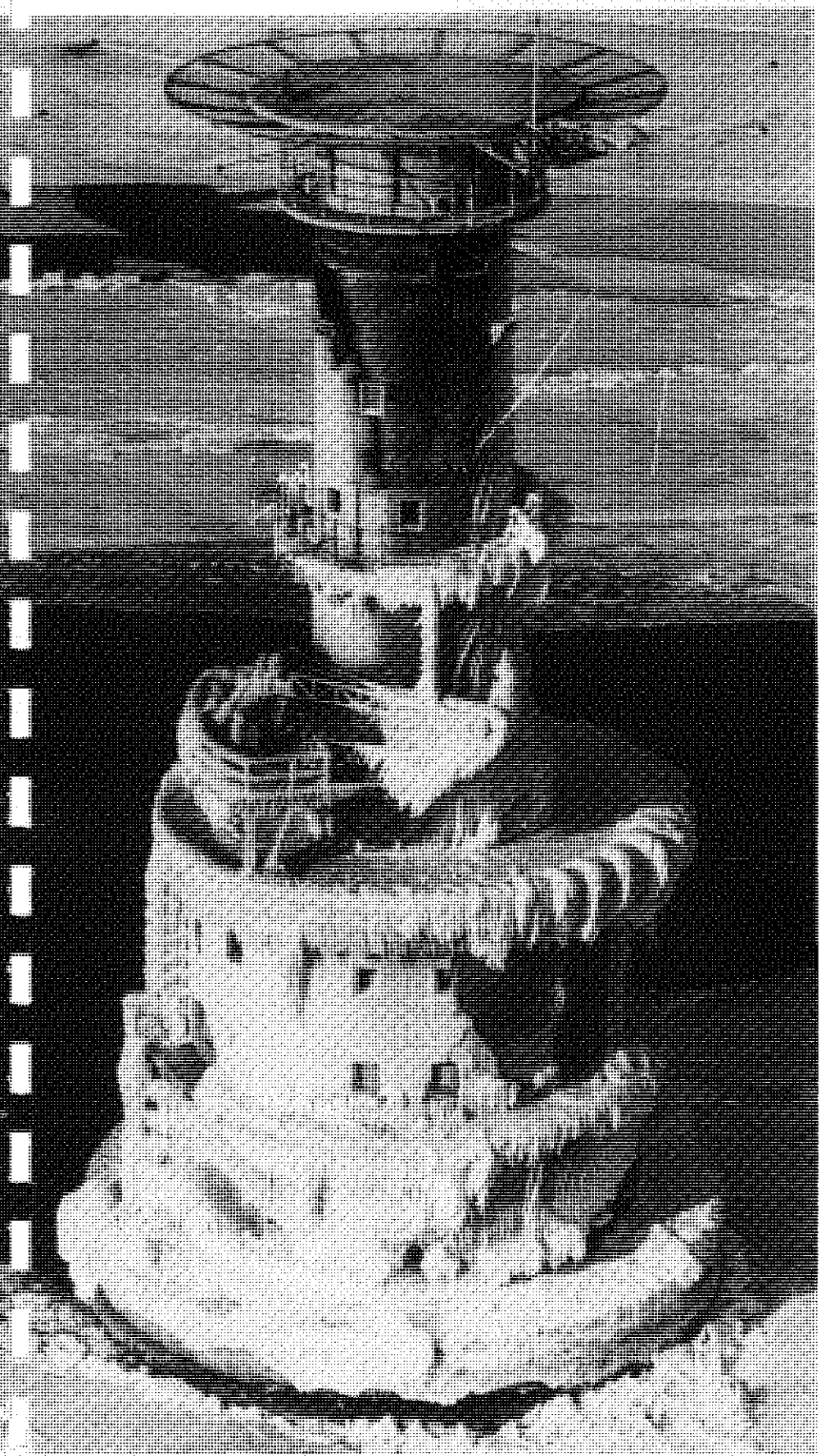

MAIN REPORT

VOLUME I

1984

VBB

VBB/Oil and Gas Division

VBB
P.O. Box 5038
S-102 41 Stockholm, Sweden Phone: +46 8 782 70 00

Report title:

IMPACT OF ICE ON
SWEDISH OFFSHORE LIGHTHOUSES

MAIN REPORT

Report date:

1984-08-30

Authors:

Jan Erik Janson, Thomas Högbom and Hans Klingenberg

Participating companies and organizations:

Amoco Production Company, USA
Exxon Production Research Company, USA
Mobil Research and Development Corporation, USA
Shell Oil Company, USA
Sohio Petroleum New Technology Development, USA
Standard Oil Company of California, USA
Norwegian Contractors, Norway
ABV, Sweden
Swedish Council for Building Research
National Swedish Board for Technical Development
Ben C. Gerwick Incorporated, USA

Distribution:

Distribution to participating companies and organizations

306dd-001a

FOREWORD

This joint industry study has been sponsored by the following companies

Amoco Production Company, USA
Exxon Production Research Company, USA
Mobil Research and Development Corporation, USA
Shell Oil Company, USA
Sohio Petroleum New Technology Development, USA
Standard Oil Company of California, USA
Norwegian Contractors, Norway
ABV, Sweden

Also two Swedish funding organizations have contributed to the financing, viz.

Swedish Council for Building Research
National Swedish Board for Technical Development

The companies have been represented in a project group that has held 2 meetings during the course of the work and 1 final meeting. Their main representatives have been

Mr Robert H. Nagel, Amoco
Dr Karl H. Runge, Exxon
Dr George C. Hoff, Mobil
Mr Paul L. Dorgant, Shell
Mr Yu Y. Hsu, Sohio
Mr Edward R. Sauve, Socal
Mr Bernt Jakobsen, NC
Mr Rolf Hörnfeldt, ABV

The Swedish Council for Building Research nominated a reference group that has held 3 meetings during the course of the work. The members are

Prof. Karl-Elis Bowin, ABV
Prof. Klas Cederwall, Royal Institute of Technology, Stockholm
Mr Kaj Lindberg, Götaverken-Arendal.

The discussions at all these meetings as well as intermediate contacts with members of the groups have been most valuable for our work.

Throughout the study, Prof. Ben C. Gerwick Jr, has been acting as adviser. He has participated at the meetings with the project group and been in continuous contact with VBB. His participation is greatly appreciated.

Stockholm August 30, 1984

Jan Erik Janson
Project Leader

OG 306dd-001
JEJ/MIA

CONTENTS

ABSTRACT

24 offshore concrete lighthouses around the Swedish coast, all of them exposed to different degrees of ice impact, have been studied with respect to ice abrasion.

In the northern Baltic, north of Lat. 60°, the ice conditions are comparable with certain areas in American Arctic.

The study includes

- Technical description of the lighthouses.
- Evaluation of available statistics on ice conditions and other environmental conditions.
- Field inspection of the lighthouses.
- Core drilling at some selected lighthouses.
- Laboratory investigation of the concrete.

The observed abrasion varies considerably between the different lighthouses. It has been possible to correlate the observed abrasion rate to ice drift velocity, ice thickness and time.

1. INTRODUCTION

1.1 Background

For offshore installations in Arctic areas, concrete offers specific advantages, as it is a comparatively easy task to design and construct concrete structures that will resist great ice forces.

The long term resistance of concrete in marine environments is in general very good, and this is borne out by experience from the North Sea installations. In Arctic areas, the impact of ice, such as ice abrasion and repeated freezing and thawing, will be added. For this reason, it is of interest to record and evaluate experience from existing concrete structures installed offshore in ice conditions similar to those in the Arctic offshore oil and gas fields. The most interesting examples of this kind of structure are probably the Swedish offshore lighthouses.

A considerable number of offshore concrete lighthouses have been installed around the Swedish coast during the last three ~~centuries~~ decades. Most of them are exposed to the impact of sea ice in the winter. Some of them are located in areas where there is ice for more than 6 months of the year, whereas others are located in areas where drifting ice dominates. Those located off the southern coast of Sweden are exposed to ice only during exceptionally cold winters. Thus, the Swedish lighthouses offer an excellent opportunity to evaluate the effects of ice impact on offshore concrete structures.

In order to investigate the effects of ice impact on the Swedish offshore lighthouses, and assess parallels with offshore concrete structures under Arctic conditions, an agreement was signed between VBB and the following companies:

- Amoco Production Company, USA
- Exxon Production Research Company, USA
- Mobil Research and Development Corporation, USA
- Shell Oil Company, USA
- Sohio Petroleum New Technology Development, USA
- Standard Oil Company of California, USA
- Norwegian Contractors, Norway
- ABV, Sweden

Funds for the project were made available partly by the above companies and partly through the National Swedish Board for Technical Development (STU) and the Swedish Council for Building Research (BFR).

1.2 Scope of investigation

The investigation has comprised all reasonably large lighthouses along the Swedish coast, with the exception of the few that have been steel-plate armoured from the time of construction and a certain number that are not exposed to the impact of ice. They cover

- different ice and water regimes,
- lighthouses of different age, with consideration given to different concrete regulations governing their construction,
- "sister lighthouses" in similar environments,
- "sister lighthouses" in different environments,

In total more than 30 lighthouses have been included in the investigation, 24 of which have been studied in detail.

The investigation has included the following five main items:

a. Data on the lighthouses

All relevant data for the lighthouses have been collected including the following:

- Year season when the lighthouse was built at the construction site.
- Year and season when the lighthouse was installed at the offshore installation site.
- Design data such as specified concrete quality (strength, cement content, cement type, additives, etc.), concrete cover, reinforcement, possible surface protection, possible repairs, etc.
- Documented data from the construction (test records, work records, diaries, etc.)
- Reports from earlier inspections of the lighthouses. Although all the lighthouses were inspected in 1974 and 1978, the effects of ice impact were, not specifically studied.

b. Ice conditions and other environmental conditions

The impact depends on several factors such as amount of ice, ice thickness, degree of packing and drift velocity. The ice conditions vary considerably along the Swedish coast and from year to year. Also local variations occur. The ice conditions have been evaluated and described.

In addition to the ice conditions, other environmental conditions such as waves, currents, sea water characteristics, etc. have been described.

c. Field investigations

c1. General inspection

All the lighthouses have been inspected ocularly and photographed, both above and below the water level. A number of of simple mechanical tools, such as hammers, chisels, scrapers and measuring rules have been used as standard equipment. In addition a covermeter has been used for measuring concrete cover; and for measuring the depth of carbonation in situ, a 3 % solution of phenolphtalein was used. The depth of erosion on the caisson wall has been checked by measuring the distance between straight-edges placed on concrete surfaces above and beneath the degraded area at the water line.

The same staff of experts, including an experienced field investigation engineer, a diver specialized in similar jobs and necessary assistants, has been engaged for the inspection of all lighthouses. During part of the time, the staff has been complemented by specialists from the Swedish Cement and Concrete Research Institute as advisers.

c2. Material sampling

After preliminary evaluation of the inspection results for all lighthouses, some of the most interesting lighthouses have been selected for thorough material quality investigation as a complement to the information collected from the construction. On a second site investigation tour, concrete cores were drilled from the selected lighthouses.

d. Laboratory investigations

The concrete cores have been analysed with respect to:

- compressive strength
- tensile strength
- density
- cement content
- chloride content
- porosity
- permeability
- freezing-thawing resistance
- micro cracks
- sulphate attack, alkali reactivity and salt crystallization

1.3 Project organization

The project work has been managed and to the major part carried out by VBB. The Swedish Meteorological and Hydrological Institute (SMHI) has been engaged for item "b" above and the Swedish Cement and Concrete Research Institute (CBI) has taken part as general advisers in items "c1" and been responsible for item "d" above. In addition, personnel from ABV have been engaged in item "c2".

1.4 Presentation and discussion of results

1.4.1 Introduction

The set of reports on the project is arranged as follows:

Volume I

- Main Report

Volume II

- Technical Description of the Lighthouses
- Ice Conditions

Volume III

- Inspection
- Material Investigation

1.4.2 Volume II

In Volume II, a presentation is given of the results from the preinvestigation phase in which all relevant data on the lighthouses have been collected and compiled. The presentation comprises general information on the design and construction of Swedish offshore lighthouses and more detailed data on the lighthouses selected for the investigation.

The ice conditions and other environmental conditions along the coast of Sweden are presented in Volume II. The waters off the Swedish coast have been divided into a number of representative areas for which ice statistics have been evaluated. For each area the occurrence and type of ice, thickness, ridges and packing have been described. More detailed statistics have been compiled for a smaller number of lighthouses covering different ice regimes, ice thicknesses and ice drift velocities. For each lighthouse, frequency tables have been compiled, indicating the relationship between different ice drift velocities and degree of ice pressure, and ice thicknesses, ice concentration and frequency of ridges. In addition, data on ice accretion and other environmental conditions such as currents, salinity, water temperature, waves and water level variations are presented.

The part of Volume II dealing with ice conditions has been prepared by the Swedish Meteorological and Hydrological Institute.

1.4.3 Volume III

In Volume III, the observations made during the field inspection of the lighthouses are presented. The surfaces of the lighthouses have been studied ocularly and photographed, both above and below the water surface. All visual damage has been measured with reference to surface area and depth.

After preliminary evaluation of the inspection results, some of the most interesting lighthouses were selected for thorough material quality investigation including material sampling. The observations made during this work are presented in Volume III.

The reports from the laboratory testing are to be found in Volume III. The major part of the laboratory testing has been performed at the Swedish Cement and Concrete Research Institute

and their report also includes a discussion chapter on the concrete quality. A separate report on thin section analysis from Teknologisk Institut, Tåstrup, Denmark is also included in Volume III.

1.4.4 Volume I

In Chapter 2 of this main report the results as reported in Volumes II and III are discussed. The possible causes of erosion depths observed are evaluated, the mechanism of ice abrasion is discussed and the possibility of predicting abrasion rate is dealt with.

In Chapter 3, conclusions are presented and recommendations for future studies are given.

In Appendix I to this main report, formation and mechanical properties of sea ice and pressure ridges are discussed. In addition, comparisons are made between the ice in the Arctic region, both first-year ice with higher salinity and multi-year ice with low salinity and greater thicknesses, and the ice affecting the Swedish offshore lighthouses, first-year ice with low salinity. The presentation is based on literature studies and is intended to be a general review of the state-of-the-art of sea ice mechanics.

In Appendix II, the impact of ice and other environmental influences on offshore concrete structures are discussed in terms of mechanisms of deterioration and control. The different impact modes discussed are chemical attack, freezing and thawing, corrosion of reinforcing steel and abrasion. The presentation is based on literature studies and is intended to be a general review of the state-of-the-art. No literature on ice abrasion has been available. Hence, the discussion on abrasion is in general terms.

2. DISCUSSION OF OBSERVATIONS

2.1 Introduction

The observations referred to are those reported in the sub-report Inspection, Volume III. They are presented in a standardized manner for all lighthouses which facilitates comparison between the different structures.

The most important observation for the discussion is the erosion depth around the water line. It is presented graphically by curves representing equal erosion depth, i.e. contour maps of the concrete caisson wall. These graphs have been prepared by computer with the raw measurement records as input. See Fig. 1 for each lighthouse in the sub-report, Inspection, Volume III.

2.2 Erosion depths observed

Erosion depths observed at the inspection of the lighthouses vary considerably along the Swedish coast and range from zero to 140 mm. Many lighthouses display no erosion at all and all of them are located south of Lat 58°30', which is about 90 km south of Stockholm. Also north of this latitude, near-shore lighthouses in sheltered waters have practically no erosion.

There is a certain amount of erosion on the concrete surfaces around the sea level on all the open sea lighthouses north of the above latitude. Between the Stockholm area; and Lat 65°, nearly all lighthouses, 8 in all, have erosion depths down to the reinforcement. Only 2 of them, however, have erosion depths deeper than the reinforcement with the reinforcement torn out from the concrete. On the other hand, these 2 display erosion depths which are many times more than the concrete cover, or 140 mm and 120 mm respectively.

As shown in Fig. 2:1, 9 lighthouses of the 24 investigated have no erosion at all, 13 of the lighthouses have erosion depths comparatively equally spread from 0 to 50 mm and these two where the reinforcement has been torn out have considerably deeper erosion. It seems reasonable to assume that the reinforcement bars could have some shielding effect as long as they are intact. In order to illustrate this, the specified concrete cover is also indicated in Fig. 2:1 for those lighthouses where the reinforcement has been exposed but not torn out.

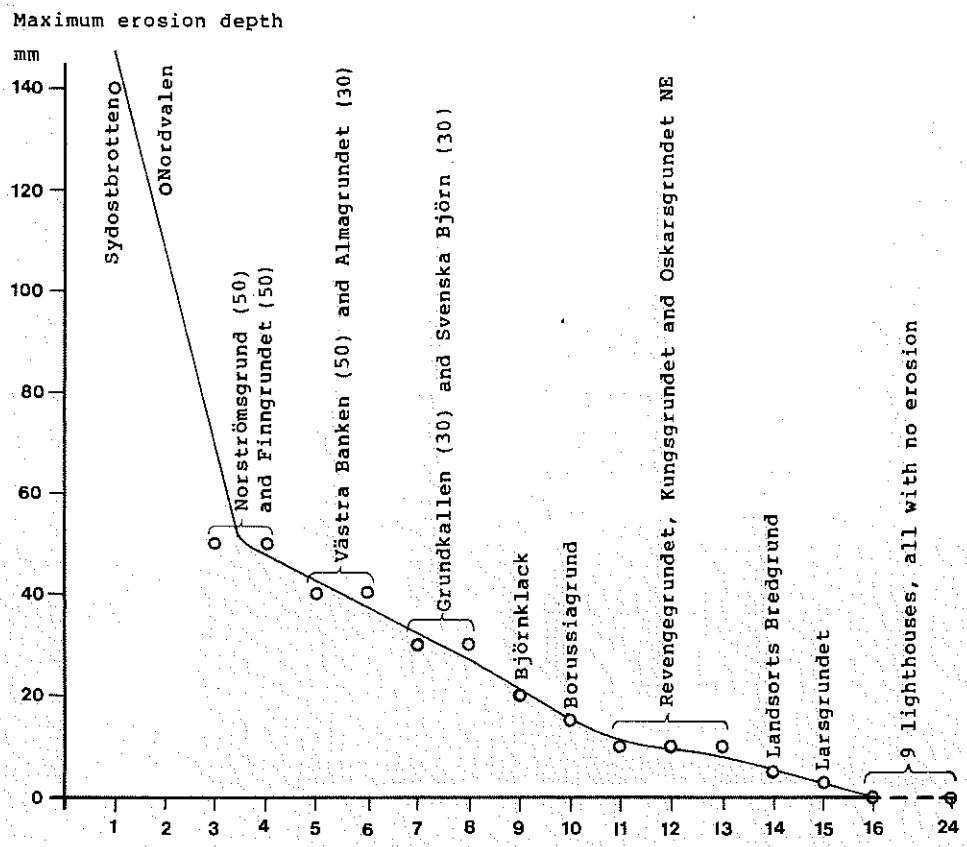

Fig. 2:1 Maximum erosion depth versus number of lighthouses with at least the maximum erosion depth.

Figures within brackets for some of the lighthouses indicate specified concrete cover.

2.3 Possible causes of erosion depths observed

2.3.1 Kind of impact

As a basis for a discussion of possible causes of the erosion depths observed, the following facts are listed:

- no erosion has been observed on lighthouses located in areas where the level ice thickness never exceeds 0.3 m,
- no erosion of any importance has been observed on lighthouses located in areas where there is fast ice throughout the whole winter,
- very significant erosion has been observed on all lighthouses located in areas characterized by close or open pack ice with ice thickness more than 0.3 m.

The conclusion to be drawn from the three facts above is that the mechanical effect of moving ice, here referred to as ice abrasion, seems to be a fundamental cause of the erosion observed.

Then, two questions should be answered:

1. Is ice abrasion the only cause of the erosion observed, or is there a combined action of ice abrasion and other environmental impact that causes the erosion?

2. What is the mechanism behind ice abrasion, and which strength parameters of the concrete have a major influence on the abrasion rate?

As regards the first question, the other kinds of impact that could possibly be of importance in combination with ice abrasion are

- freeze-thaw action
- temperature gradients
- chemical attack
- adfreeze

Freeze-thaw action

All lighthouses are exposed to cyclic freezing-thawing in the winter season. Damage of a kind that is typical for freeze-thaw impact has, however, only been observed to a very small extent. The main impression is that the lighthouses have resisted freeze-thaw impact very well.

On the other hand, the freeze-thaw resistance as measured by the standard freeze-thaw test method is not to be regarded as acceptable for structures in a severely exposed environment. See the material investigation report in Volume III. About half of the test specimens do not fulfil the requirements stipulated in Sweden for concrete which should resist freezing and thawing with de-icing salts. In fact, the freeze-thaw resistance is lower for the two worst eroded lighthouses than for the other two included in the material investigation.

The possible mechanism behind a combined action of abrasion and freeze-thaw, which explains why no typical cases of freeze-thaw damage are observed on the surfaces above the saturated zone, would be the following.

The saturated concrete between low and high water is much more prone to fail when exposed to freeze-thaw action than the concrete on higher elevations which is never completely saturated. Freeze-thaw attack initially shows up as multiple micro and sub-macro cracking concentrated primarily at the surface, where the concrete is unconfined. If then the concrete surface is struck by moving ice, or if the ice is crushed against the surface, the abrasive effect is greater than if no cracking from freezing-thawing had taken place.

However, the fact which really demonstrates that freeze-thaw action can hardly be of any great importance is that the majority of the erosion has occurred below the water surface, where no freze-thaw action is possible.

Temperature gradients

The question has been raised of whether or not the temperature gradients close to the water surface could contribute to the erosion observed. The air temperature can quite often fall to below -30°C in the northern Baltic area, and the caisson wall of the lighthouses will then be exposed to tensile stresses due to restricted temperature contraction as it is kept at about 0°C below the water line.

A temperature decrease of 30°C means a tensile strain on the concrete of about 0.3 o/oo, if the concrete is completely restricted from contraction. As the tensile limit strain is only 0.05-0.15 o/oo, cracks will appear.

For the lighthouses, however, it is not likely that the concrete will be strained to the above degree due to temperature gradients, as there will always be only a partial contraction restriction. Furthermore, if the strain should exceed the tensile limit strain resulting in temperature cracks, such cracks could hardly be of any importance for the erosion of the concrete surface, because the cracks would be in the macro scale with solid unaffected concrete between them.

In addition, temperature gradients do not occur under the water surface, where most of the erosion has been found.

Chemical attack

Chemical attack on the concrete surfaces from sea water is normally caused by sulphate ions or magnesium ions. In the Baltic Sea, however, the average ion concentrations in kg/m^3 are only 0.58 and 0.26 respectively for sulphate and magnesium, which is about a quarter of the corresponding figures for the North Sea. In the case of the Bothnian Sea and the Gulf of Bothnia the figures are even lower.

It was also confirmed in the laboratory testing of drilled-out cores that practically no chemical attack has occurred. Only very superficial sea water impact was noticed visually on the outer surfaces of the cores, and never extending deeper than 3 mm from the surface. The impact could only be observed by a small change in colour. No sign of sulphate attack or any defects due to alkali-aggregate reactions were observed.

Consequently, chemical attacks cannot have had any influence on the erosion that was found.

Adfreeze

It has been discussed whether or not adfreeze could be a factor that contributes to the erosion observed. The mechanism would then be that an ice sheet is adhered to the structure by freezing. When movement starts, the bond between ice and concrete is broken, and the question is then whether concrete particles from the surface are broken loose.

This question has been raised especially in connection with lighthouses located in areas with landfast ice where vertical movements caused by changes in sea level occur. Larsgrundet is a typical example of this kind of lighthouse. Practically no erosion has been observed.

The most significant erosion has been observed where the ice characteristics include high ice drift velocities. Then, adfreeze can hardly be a factor to consider.

2.3.2 Mechanism of abrasion

For an understanding of possible ice abrasion mechanisms on concrete a comparison should be made between the mechanical properties of ice and concrete.

Fig. 2:2 shows stress-strain curves for concrete and ice in the same diagram. The curves are typical examples but considerable variations from the curves could occur in practice.

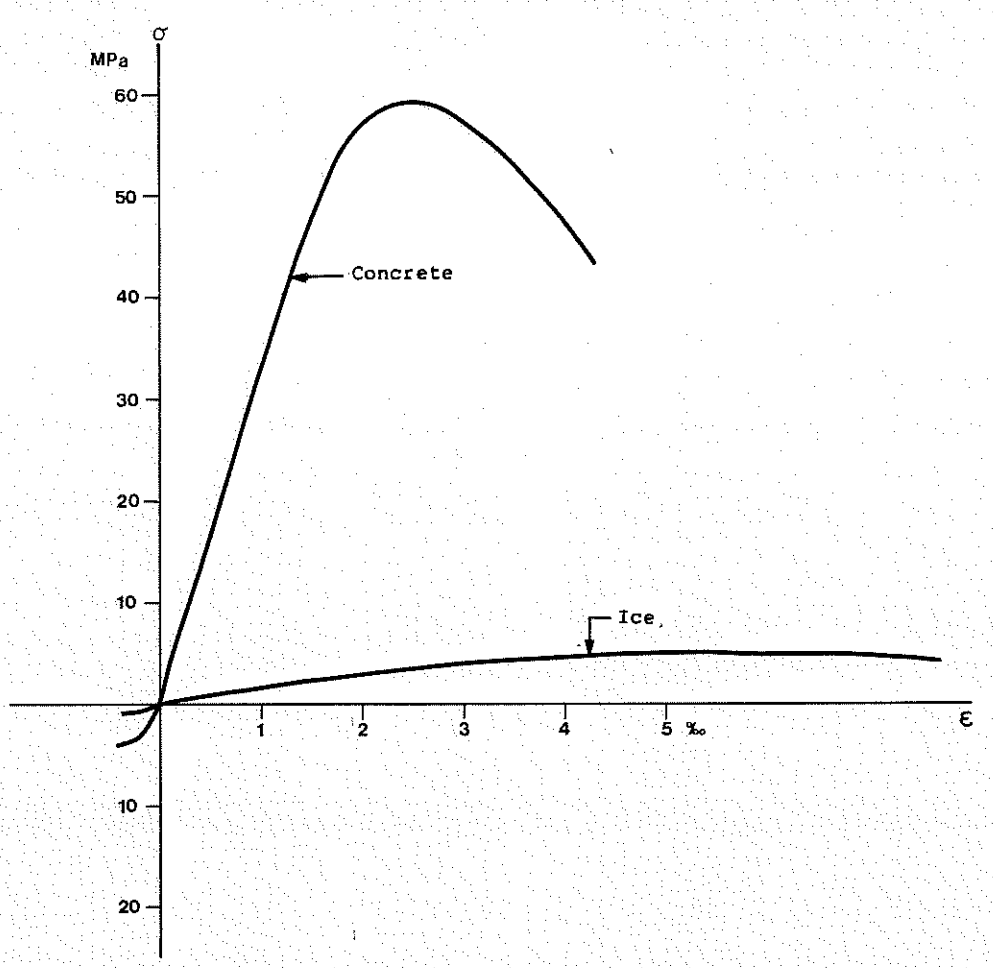

Fig. 2:2 Typical stress-strain curves for high strength concrete and Baltic Sea ice.

The ice curve in Fig. 2:2 indicates a compressive strength of 5 MPa. The compressive strength of Baltic Sea ice, Schwartz (1971), varies between 2 and 10 MPa depending on temperature at a strain rate of 1 to 10 o/oo/sec. The ice curve in Fig. 2.2 thus represents approximately the stress-strain relationship when Baltic Sea ice is compressed from zero to crushing during a period in the range of 0.5 to 5 sec.

The concrete curve in Fig. 2:2 is an example of the stress-strain relationship of a high strength concrete. The compressive strength indicated by the curve is about the same as that found for the lighthouses covered by the material investigation in Volume III. Also for concrete, the stress-strain relationship is influenced by the strain rate but to a smaller extent. The curve in Fig. 2:2 represents a strain rate of about 1 o/oo/h. For higher strain rates, the strain at max stress is somewhat lower than the 2.5 o/oo shown in Fig. 2:2, down to a little less than 2 o/oo. Thus, for the same strain rate for both ice and concrete the curves are even more different from each other than shown in Fig. 2:2.

The question now arises as to how ice, which is so much softer and weaker than concrete, as illustrated by Fig. 2:2, can have an abrasive effect on concrete to the extent observed in this study. There are, however, a number of aspects that must be considered.

First, it should be observed that the concrete curve in Fig. 2:2 is valid for a piece of concrete that is of sufficient size for the constituents of the concrete, i.e. aggregate, sand and cement paste, to interact in an effective way. If the concrete specimen tested is so small that the load transfer through the specimen is very much dependent on the location of the individual pieces of aggregate relative to the specimen boundaries, the stress-strain relationship varies considerably and cannot be expressed by a single curve. See Fig. 2:3.

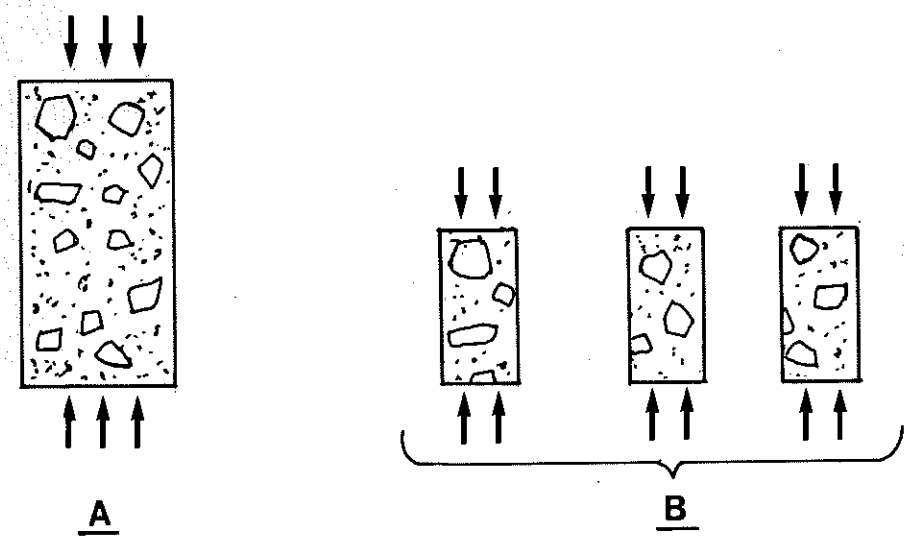

Fig. 2:3 The influence of test specimen size on load transfer through the specimen.

A. Ordinary size specimen with a width of several times that of the largest pieces of aggregate. In this case the test results are reasonably reproducable.

B. Small size specimens in which the location of the aggregate fractions will have an influence on the test results. The scatter between the test results from such small specimens will be considerable.

Where drifting ice hits the concrete surface, the area of contact between ice and concrete varies constantly as the ice moves and crushes. A very small area of contact increases the crushing strength of the ice due to a high degree of confinement. A very small area of contact also means a strength increase due to confinement in the case of the concrete but another effect is that the peak value of contact pressure moves over the concrete surface and hits individual pieces of aggregate or, alternatively, cement mortar areas, see Fig. 2:4. The effect of this is similar to the case when insufficiently large specimens are used for testing; the apparent strength varies so that the strength difference between concrete and ice is occasionally much lower than shown in Fig. 2:2.

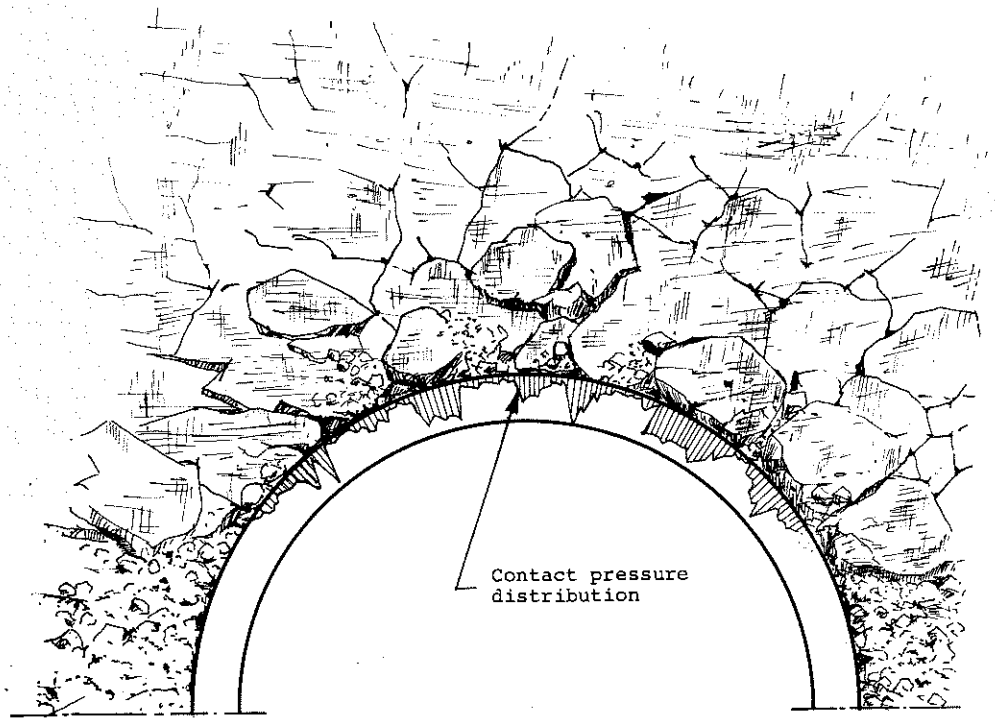

Fig. 2:4 The contact pressure between ice and structure. The pressure distribution is uneven with pronounced peaks that change due to the moving and crushing of the ice.

A further aspect other than differences in concrete strength between local spots on the concrete surface is that, after the concrete surface has become rough due to non-uniform abrasion, the ice can strike the concrete from different directions, i.e. not only perpendicular to the surface. It was observed that at the lighthouses with measurable erosion around the water line, the aggregate stones were exposed and to some extent protruding from the surface. The cement mortar had obviously been scraped off. See Fig. 2:5.

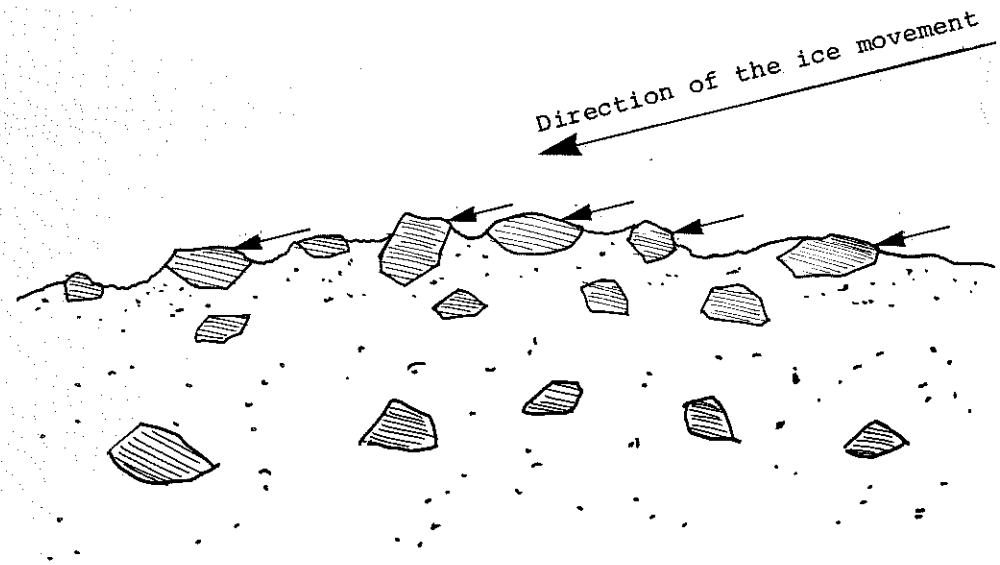

Fig. 2:5 Protruding aggregate stones are exposed to forces from moving ice from varying directions, i.e. not only perpendicular to the concrete surface.

A force acting on the side of a protruding part is much more effective than a force acting perpendicular to the surface.

A third aspect of how ice can have an abrasive effect on concrete in spite of the great difference in strength as illustrated in Fig. 2:2 is that fatigue may play a role in reducing the strength of the concrete (although not that of the ice). Again, it is important to consider that concrete is not a homogeneous material. On the basis of what is known about the fatigue strength of concrete as experienced from laboratory tests, a possible second concrete curve in Fig. 2:2 that connects points indicating stress and strain after a large number of stress cycles, will not be so very much lower than the concrete curve shown, that it will be comparable to the ice curve. However, when local areas between the aggregate stones are considered, the case is different. Then also the presence of microcracks and variation in bond between cement mortar and aggregate stones may influence the occurrence of local failure due to fatigue. It is particularly probable that the cyclic loading effect associated with the change of both magnitude and direction of ice loads on protruding parts will significantly reduce the strength. Variation of the direction of the forces on the aggregate stones in Fig. 2:5 will have a rocking effect on the stones that increases the rate by which they come loose due to the ice impact.

From the above, it is clear that the expression "ice abrasion" covers a rather complex mechanical interaction of ice impacting on a concrete surface, where the concrete strength, as determined by standard concrete strength test procedures, does not directly define its abrasion resistance. Consequently, most probably, abrasion resistance with respect to other forms of abrasion than ice abrasion, e.g. abrasion of a concrete floor or a concrete road surface from the action of tyres, abrasion of a concrete surface from a high velocity water stream in a spillway or abrasion inside a concrete pipe from suspended sand, is not directly related to the resistance to ice abrasion.

The question on the true mechanism of ice abrasion is important for the possibility to perform accelerated laboratory ice abrasion tests. The mechanism of ice abrasion must also be understood in order to judge whether other kinds of concrete such as lightweight aggregate concrete can be used in areas where ice abrasion is a concern.

2.4 Abrasion rate

The abrasion rate expressed as maximum erosion depth divided by number of years after installation has been evaluated for the lighthouses. See Table 2:1. The details behind Table 2:1 are given in the sub-report Inspection, Volume III.

Lighthouse	Maximum erosion depth mm	Number of years after installation	Abrasion rate mm/year
Larsgrundet	3	19	0.2
Björnklack	20	14	1.4
Borussiagrund	15	14	1.1
Norströmsgrund	50	12	4.2
Nordvalen	120	22	5.5
Sydostbrotten	140	20	7.0
Finngrundet	50	14	3.6
Västra Banken	40	12	3.3
Grundkallen	30	24	1.3
Svenska Björn	30	15	2.0
Revengegrundet	10	22	0.5
Almagrundet	40	19	2.1
Landsorts Bredgrund	5	11	0.5
Kungsgrundet	10	27	0.7
Oskarsgrundet NE	10	22	0.5
Gustaf Dalén	0	16	
Dämman	0	16	
Ölands Södra Grund	0	32	
Blenheim	0	8	
Falsterborev	0	11	
Oskarsgrund SW	0	22	
Svinbådan	0	24	
Fladen	0	14	
Trubaduren	0	17	

Table 2:1 Observed abrasion rate expressed as maximum erosion depth divided by number of years after installation

Now, the main question is whether the abrasion rate can be correlated to environmental parameters in a way that makes it possible to draw any conclusions from this investigation when designing offshore concrete structures in other areas.

From the discussion above on possible causes of erosion it is evident that the main cause is the mechanical impact of moving ice. The lighthouses are exposed to considerable numbers of small ice floes striking their concrete surfaces

with varying velocity. Another kind of impact is that of large ice floes which are crushed against the concrete surface of the lighthouse.

As an example of ice impact, Fig. 2:6 (page 2:13) shows the Norströmsgrund lighthouse in the winter 1981. This lighthouse is equipped with accelerometers and videocameras that are automatically started when the lighthouse responds to the ice impact imposed by a certain acceleration.

A more typical example of a case where the crushing of the ice is the dominant form of energy dissipation when a fixed structure counteracts moving ice is illustrated on Fig. 2:7 (page 2:14). It shows the Grundkallen lighthouse protruding through a vast sheet of ice.

Before presenting the observed abrasion rate against parameters such as ice drift velocity, ice thickness and number of days per year with a certain ice drift velocity and a certain ice thickness, it is of interest to discuss possible relations between the parameters from a purely theoretical point of view.

Two basically different extreme cases can be distinguished with respect to how the kinetic energy of the ice floes is dissipated. One case is where the retardation of the floes against the structure causes peak forces. The other case is where the energy dissipation is associated with the ice crushing against the concrete structure and where the ice floes are so large that the structure does not really have any influence on the ice floe velocity.

In the first extreme case, the loss of concrete by abrasion per time unit should be proportional to the dissipation of kinetic energy per time unit. Thus the kinetic energy of the ice floes, i.e. $mv^2/2$, per time unit should be summed up. The mass, m, of an ice floe is proportional to its thickness, s. The number of ice floes per time unit that hit the structure is proportional to the velocity, v. Consequently, the loss of concrete by abrasion per time unit should be proportional to v^3s. In this discussion, it is assumed that all ice floes have about the same size, or at least, that the size is not correlated to the thickness. It is also assumed that the number of ice floes per areal unit is not depending on the velocity. As ice abrasion is defined as abrasion depth and not loss of concrete, the proportionality factor, v^3s, should be divided by s resulting in v^3 as the proportionality factor between ice abrasion rate and ice character-

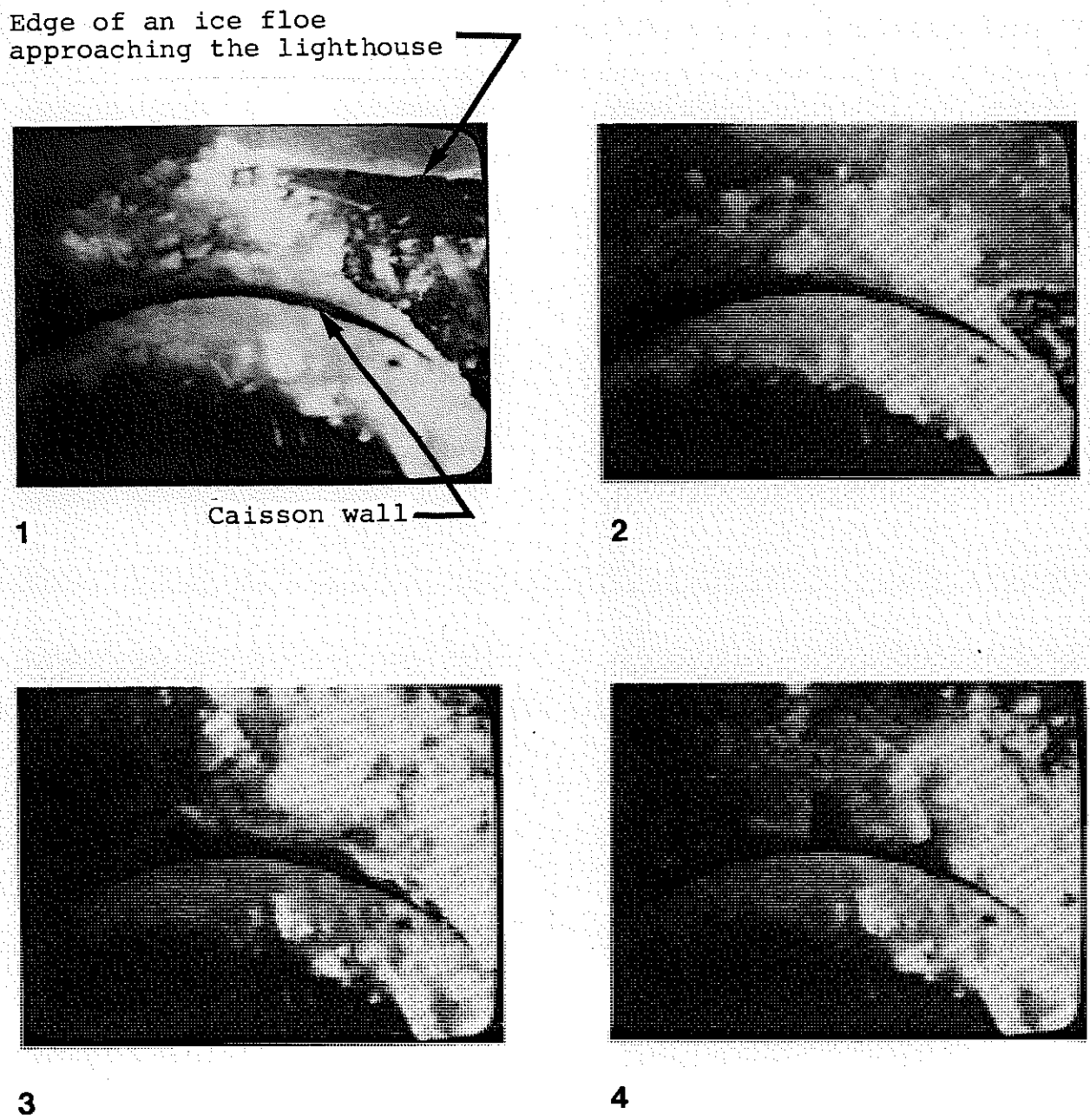

Fig. 2:6 The Norströmsgrund lighthouse. The photos show how an ice flow approaches the lighthouse and crushes against the caisson wall. The time interval between the photos is 24 s.

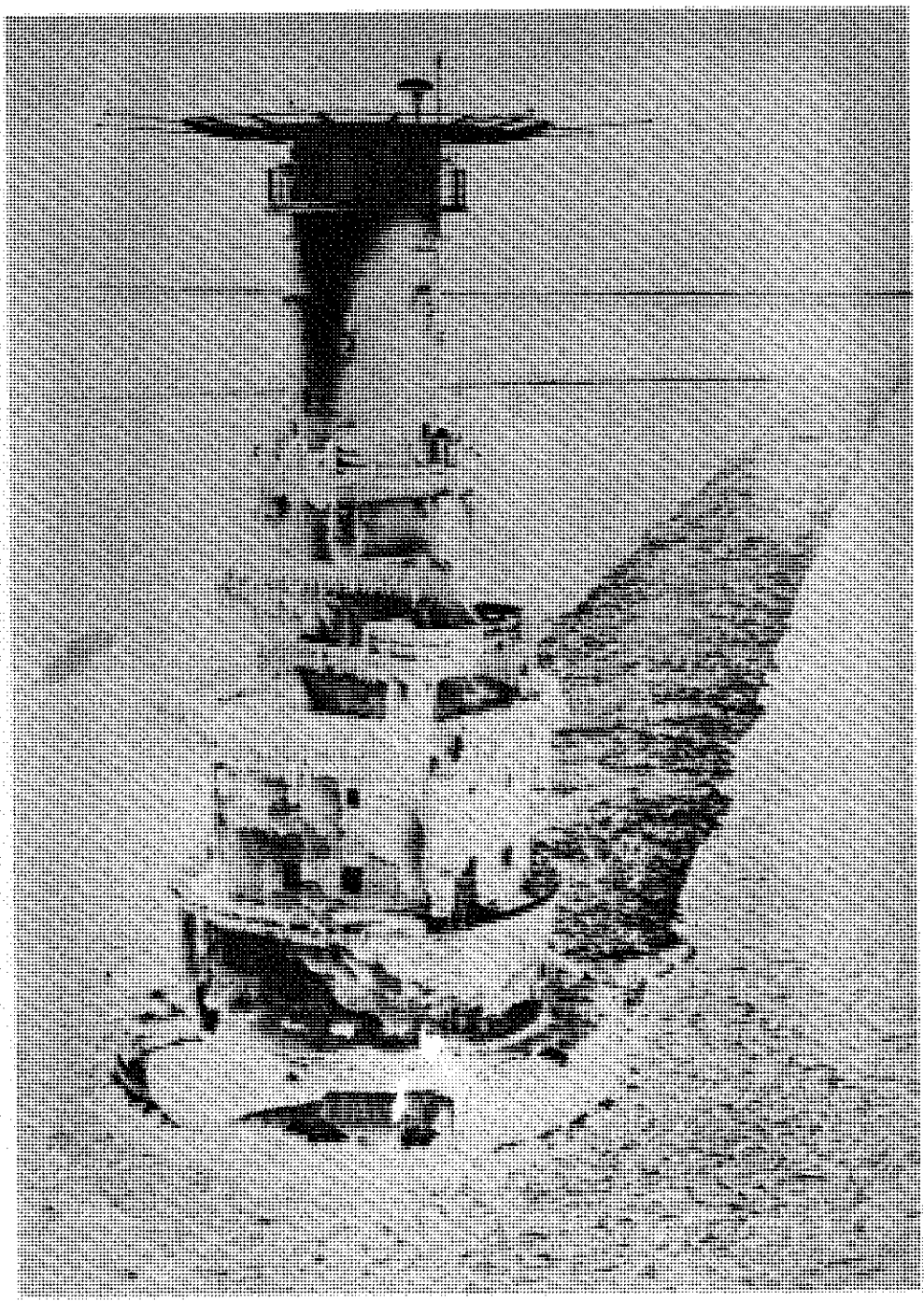

Fig. 2:7 The Grundkallen lighthouse forced through a big moving ice sheet.

istics. The abrasion rate defined as abrasion depth per year should be proportional to $\int v^3 \, dt$ integrated over a year.

Naturally, only ice floes with a certain minimum thickness should be included in the integration. It is obvious that excessively thin ice floes will break when hitting the structure, while a thicker ice floe with the same size and velocity will not break.

In the second extreme case, which better corresponds to observations of the ice behaviour, the ice velocity is not affected by the fixed structure. The ice breaks against the structure which is forced through the ice. The loss of concrete per time unit should then be proportional to the energy dissipation associated by the breaking of the ice.

Two possibilities can then be distinguished. If the ice breaks in pure crushing, the strength of the ice is proportional to the thickness, s. If the ice breaks by buckling, the strength of the ice is proportional to the thickness powered to approximately 2 (in analogy with buckling of a bar on an elastic foundation). The loss of concrete should then be proportional to s or s^2 depending on failure mode.

The ice velocity, v, is applied linearly if the influence of strain rate is not taken into account. If the ice strength is assumed to increase linearly with increasing strain rate, the ice velocity should be squared, v^2.

Thus, in the case where the ice velocity is not affected by the fixed structure, the loss of concrete should be proportional to $v\,s$, $v\,s^2$, $v^2\,s$ or $v^2\,s^2$, and the abrasion depth proportional to v, $v\,s$, v^2 or $v^2\,s$ or, of course, all intermediate combinations, $v^a\,s^b$, where $1 \leq a \leq 2$ and $0 \leq b \leq 1$. The abrasion depth per year should be proportional to $\int v^a\,s^b \, dt$.

The above discussion on the proportionality factor of the abrasion rate can be summarized as follows

I. If the ice floes are rather small and thick:

   Proportionality factor v^3

II. If the ice floes are large and thick (so that pure crushing occurs) and the velocity is small (so that the ice strength increases significantly with increasing strain rate):

   Proportionality factor v^2

III. Similar to II but with a higher ice velocity (so that no significant strength increase occurs when the strain rate increases):

Proportionality factor v

IV. If the ice floes are thinner (so that the ice breaks by buckling) and the velocity is small (so that the elasticity modulus increases significantly with increasing strain rate):

Proportionality factor v^2 s

V. Similar to IV but with higher ice velocity (so that no significant increase in elastic modulus occurs when the strain rate increases):

Proportionality factor v s.

The time intervals between the photos in Fig. 2:6 are 24 sec.The camera takes a photo every 8 sec., so there are two photos taken during the intervals between the photos shown in Fig. 2:6. The average ice drift velocity during the interval between photos 1 and 2 is 0.12 knots, between photos 2 and 3 0.10 knots and between photo 3 and 4 0.04 knots. Thus, in this particular case, the velocity is considerably reduced when the ice floe hits the lighthouse. Then, at a reduced velocity, crushing of the ice flow occurs. This means that Fig. 2:6 illustrates a case that is between the two extreme cases mentioned above. Part of the kinetic energy of the ice flow is dissipated by retardation and the remaining part is dissipated by crushing. As is shown in the following, the crushing of the ice is the dominating factor that causes ice abrasion.

Although the current investigation only includes field observations of abrasion on one occasion, i.e. in the summer 1983, it is possible to make an approximate evaluation of the abrasion rate for each lighthouse as an average over all years after installation and to compare this average abrasion rate with available data on observations of ice thickness and ice drift velocity.

The sub-report Ice Conditions and Other Environmental Conditions, Volume II, includes frequency of ice thickness in certain ice drift conditions as observed in the winter 1978/79 at most of the lighthouses off the east coast of Sweden (Tables 4-12 in the sub-report). These tables include observations at the lighthouses from

the north end of the Gulf of Bothnia down to Lat 58°30' south of Stockholm. The sub-report also includes the same kindof observations at lighthouses further south and off the west coast of Sweden, but these structures are not of interest with respect to ice abrasion.

Using Tables 4-12 in the sub-report on ice conditions, the number of days with a certain ice thickness and a certain ice drift velocity during the winter 1978/79 has been evaluated.

As the ice abrasion that occurred in the winter 1978/79 is not known but only the total ice abrasion since installation of the lighthouses, which after division by the number of years after installation can be regarded as average abrasion rate, the specific information on ice conditions in the winter 1978/79 can not be used directly. Therefore, since the total number of days that each lighthouse has been subjected to ice conditions each winter since installation is known, the number of days with specific ice thickness and ice drift velocity in the winter 1978/79 have been multiplied by (average number of days in ice)/(number of days in ice in the winter 1978/79). This means that it is assumed that although the number of days in ice in the winter 1978/79 may differ from the average, the relative frequencies of different ice drift velocities and ice thicknesses do not change very much from year to year.

In this way the following quantities have been calculated

I $\int v^3\,dt$
II $\int v^2\,dt$
III $\int v\,dt$
IV $\int v^2 s\,dt$
V $\int vs\,dt$

to verify the theoretical discussion above.

In order to provide an overall picture the following quantities have also been calculated

$$\int dt$$
$$\int s\,dt$$
$$\int v^2 s^2\,dt$$
$$\int vs^2\,dt$$
$$\int s^2\,dt$$

The coefficients of correlation between all the above integrals and the observed abrasion rates from Table 2.1 have been calculated and are presented in Fig. 2:8.

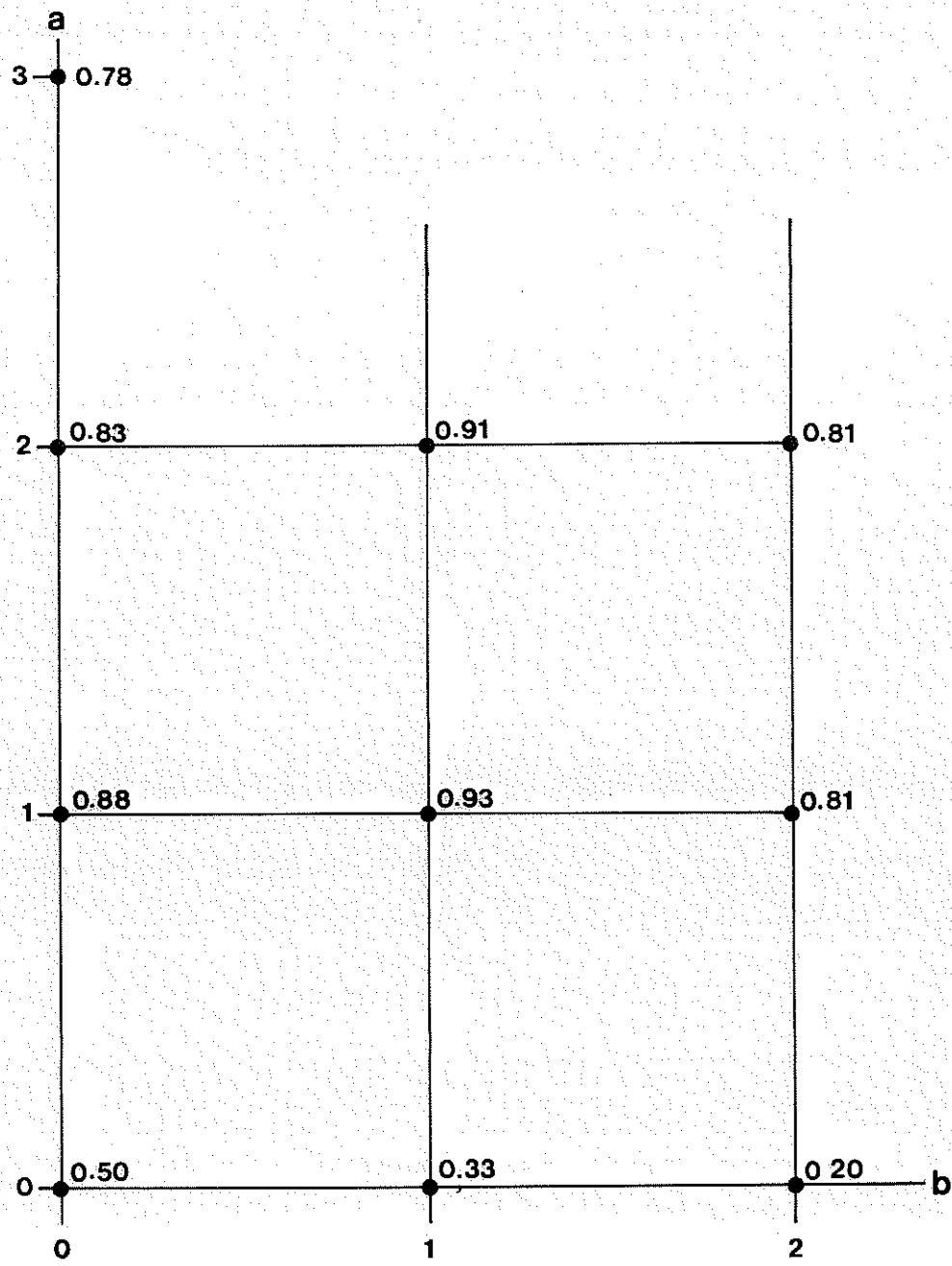

Fig. 2:8 Coefficients of correlation between abrasion rate and $\int v^a s^b dt$ for the lighthouses off the Swedish east coast north of Lat 58°30'.

From Fig. 2:8 it can be seen that the highest value of the coefficient of correlation between the observed abrasion rate and $\int v^a s^b dt$ is reached when a and b are chosen in the following intervals: $1 \leq a \leq 2$ and $0 \leq b \leq 1$.

Figs 2:9-12 show the observed abrasion rates as functions of $\int v\,dt$, $\int v^2\,dt$, $\int vs\,dt$ and $\int v^2 s\,dt$ respectively. In each figure, the straight line that best fits the observations, the regression line, is also shown.

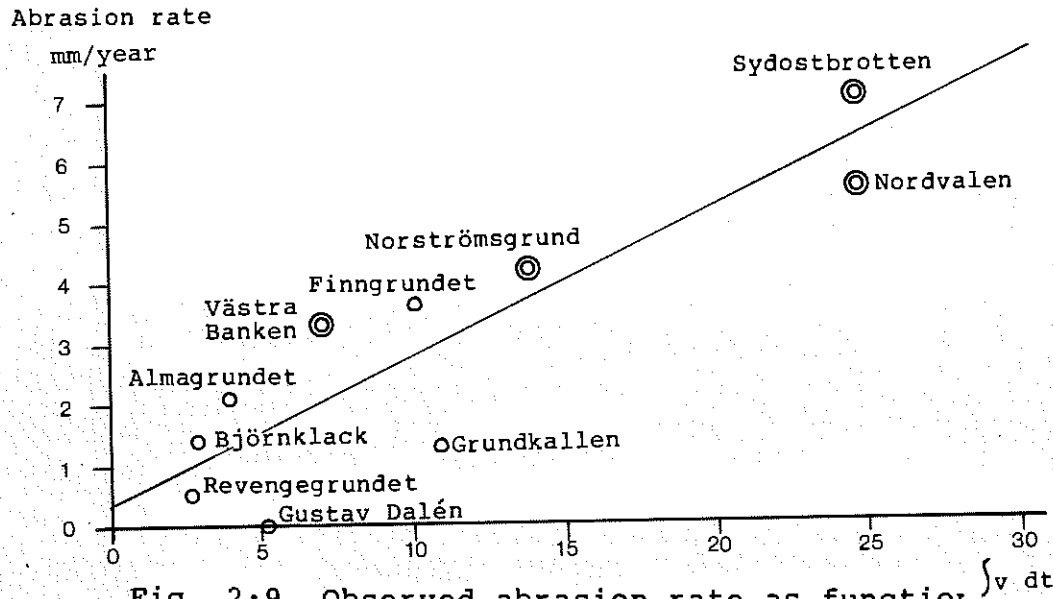

Fig. 2:9 Observed abrasion rate as function of $\int v\,dt$.

Abrasion rate is defined as abrasion depth per year. The integration is made over one year.

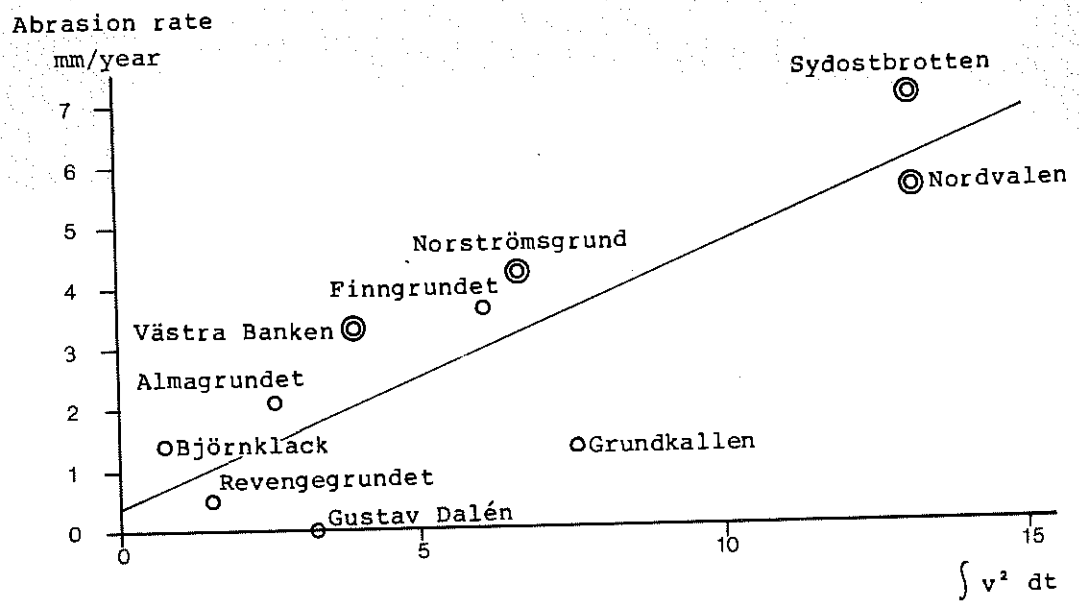

Fig. 2:10 Observed abrasion rate as function of $\int v^2\,dt$.

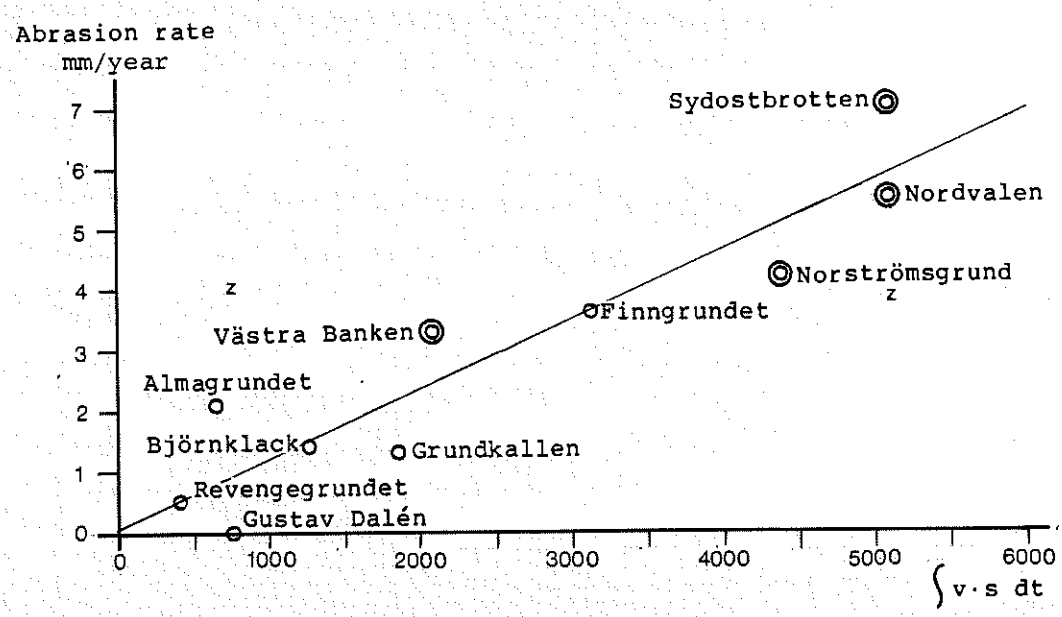

Fig. 2:11 Observed abrasion rate as function of $\int vs\ dt$.

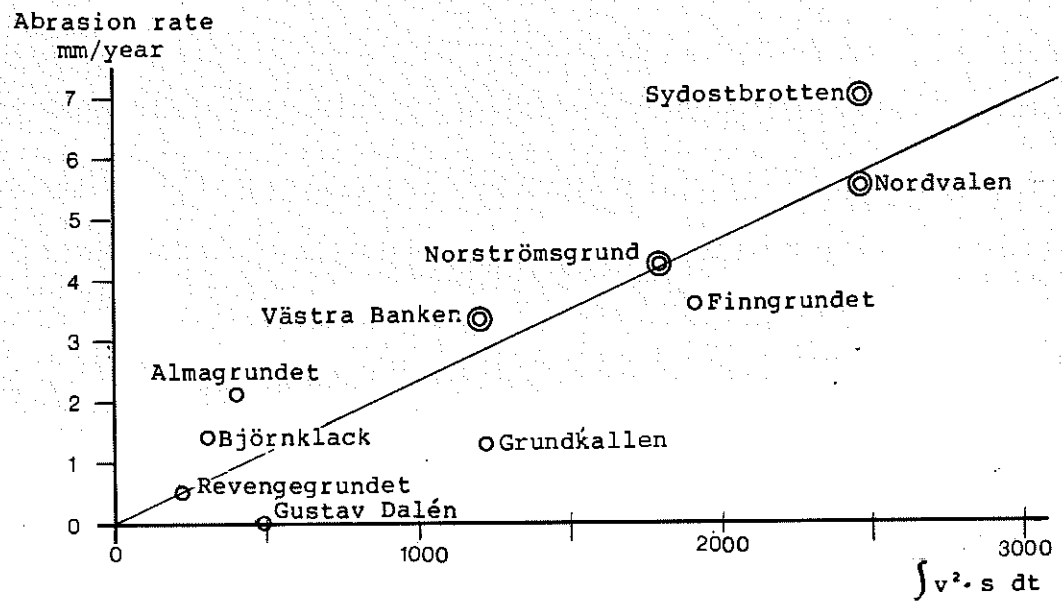

Fig. 2:12 Observed abrasion rate as function of $\int v^2 s\ dt$.

The ligthouses indicated by double circles in Figs 2:9-12 are those from which cores have been drilled and laboratory tested. See sub-report Material Investigation, Volume III.

One cause for uncertainty regarding the above relation between abrasion rate and ice characteristics is that the direction of the ice drift is not taken into account. No detailed information is available, on ice drift direction;only ice drift velocity. This means that if the ice drift direction is more variable at some of the lighthouses than the others, the abrasive effect of the ice has been underestimated for these lighthouses.

A remark which can be made regarding all Figs 2:9-12 is that Gustav Dalén and Grundkallen are those lighthouses for which the observed abrasion rates fall below the regression line to the greatest extent.

As far as Gustav Dalén is concerned one could suspect that the ice condition data used in the evaluation is more inaccurate than for most of the other lighthouses. There are less yearly variation in ice conditions in the northern part of the Baltic than south of Stockholm. Gustav Dalén is the lighthouse that is located furthest to the south of the lighthouse included in Figs 2:9-12.

Regarding Grundkallen one should observe that the specified concrete cover is only 30 mm and that the reinforcement bars are intact. They could thus have had a shielding effect and protected the concrete behind the reinforcement layer from ice abrasion. The ice at Grundkallen is thinner than at Sydostbrotten and Nordvalen where the reinforcement bars have been torn out. This may explain why the reinforcement has resisted the ice forces.

The v, s and t values for Sydostbrotsten are not based on measurements performed at the specific site, as they are for the other lighthouses. Instead, the values for Nordvalen, that is located near Sydostbrotten, have been used also for Sydostbrotten.

3. CONCLUSIONS AND RECOMMENDATIONS

3.1 Conclusions

The investigation comprises the detailed mapping of damage around the water line of the lighthouses as observed in the summer 1983. This damage appears as erosion of the concrete surface with erosion depths varying from 0 to 140 mm. As explained in Chapter 2, the erosion is caused by impact from moving ice and therefore the term ice abrasion will be used, although the mechanism behind the damage would be more accurately defined as crushing and spalling of concrete and aggregate than pure abrasion.

Abrasion rate is defined as depth of abrasion per year. The observed abrasion rate is simply the observed maximum depth of abrasion divided by the number of winter seasons after installation of the lighthouse. In order to investigate how much abrasion has occurred during a particular winter season, continued studies should be done where selected lighthouses are continuously studied in order to follow up the ice abrasion from year to year.

The observed abrasion rate has been found to be approximately proportional to $\int v^a s^b \, dt$ distributed over the whole winter season. The values of a and b shall be chosen in the intervals $1 \leq a \leq 2$ and $0 \leq b \leq 1$. See Fig. 2:8

If only integers are considered for a and b the combinations should be ranked as follows according to Fig. 2:8:

1. a = 1 b = 1
2. a = 2 b = 1
3. a = 1 b = 0
4. a = 2 b = 0

All these combinations of a and b have their own value for slope and intercept of the straight line that best fits the observed values of abrasion rate.

As a preliminary conclusion, combination 1 above, a = b = 1, is recommended. The reason for this is as follows:

First, it gives the highest degree of correlation with the observations (closely followed by combination 2).

In addition, it also corresponds best to the theoretical discussion that proceeds Fig. 2:8 in Chapter 2. According to this, combination 1 is valid if the ice is thin enough to fail in buckling instead of pure crushing and if the velocity is high enough that no significant increase in ice failure load will occur if the velocity increases further.

If the ice strain rate is higher than about 0.5 o/oo/sec., there is practically no further increase in ice strength at increasing strain rate. The ice drift velocity is related to the strain rate as follows $\dot{\varepsilon} = v/2D$ where D is the diameter of the lighthouse. Consequently, the above expression for the abrasion rate should not be used if the velocity is lower than 0.5 2D/1000 = D/1000 m/sec (D in m). For D = 20 m, the velocity should not be lower than 0.02 m/sec.

With respect to ice thickness there is most probably a limit above which no increase in ice abrasion occurs if the ice thickness increases further. For thicker ice combination 3 should then be used. It is likely that this limit is around 1 m or somewhat below.

Using combination 1, the straight line that best fits the observed abrasion rates as a function of $v\ s\ dt$ is:

$$\text{Abrasion rate (mm/year)} = 0.00114 \int vs\ dt + 0.08$$

where v = ice drift velocity in knots
s = ice thickness in mm
t = time in days

For the sake of simplicity and in order to cover the majority of observations, the following expression is recommended for ice abrasion predictions:

$$\text{Abrasion rate (mm/year)} = 0.0015 \int vs\ dt.$$

See Fig. 3:1.

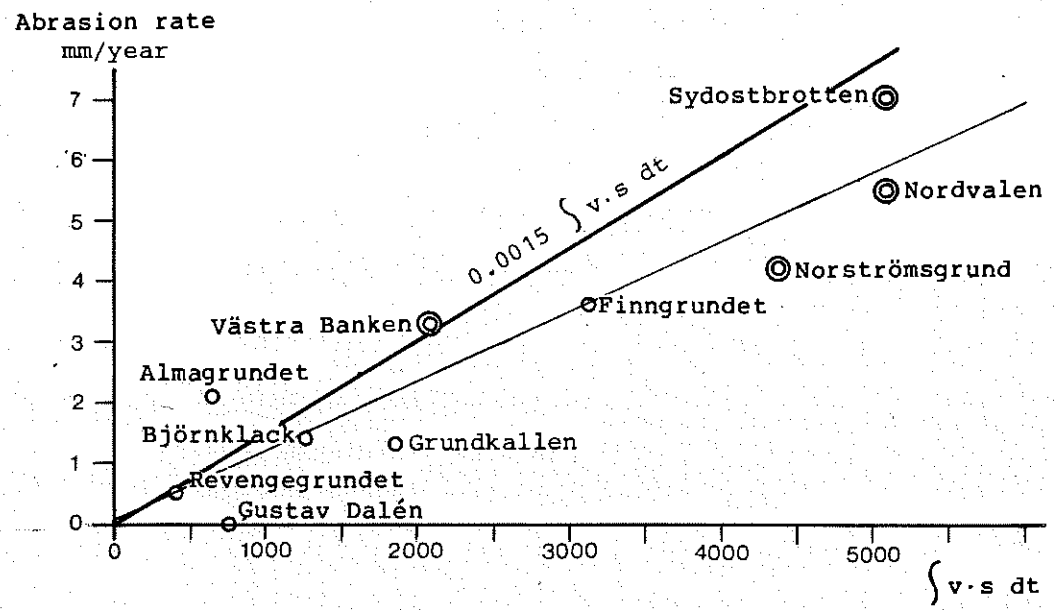

Fig. 3:1 Observed abrasion rate as function of $\int vs\,dt$. Recommended relation for ice abrasion predictions indicated.

Only one lighthouse has an abrasion rate that exceeds this line and it displays only very moderate abrasion. It is characterized by very low s and rather high v.

This means for example that if the ice movement is concentrated to 30 days every year with a constant velocity of 0.2 knots and a constant ice thickness of 800 mm the abrasion rate is

0.0015 0.2 800 30 = 7.2 mm/year

The uncertainties involved in using the above expression to predict abrasion rate for offshore structures are of two kinds. One such uncertainty is whether the expression provides a reasonable reflection of the abrasion rate in the Baltic, i.e. if this investigation has clarified to a sufficiently accurate degree how the Baltic Sea ice influences the marine concrete structures in the area. In Chapter 2, the results of the investigation have been discussed with regard to the abrasion on the actual lighthouses. In addition to what is mentioned in Clause 2.4 it should be pointed out that the size and shape of a structure probably have an influence on the abrasion rate. The results of the investigation should only be referred to when dealing with vertical walled structures with circular cross section at the water line with diameters in the range of 5-25 m.

The other kind of uncertainty is associated with applying experience from the Baltic when ice abrasion in other areas is to be predicted. No comparative field studies in other areas are included in this investigation. Therefore, the only way to draw any conclusions on abrasion rate in an area other than the Baltic is to combine the field observations on abrasion rate in the Baltic with known facts about ice mechanics.

In Appendix I, a brief resumé is presented of the fundamental ice mechanics based on literature studies. Appendix I also includes relevant information on Baltic Sea water and Baltic Sea ice.

The main conclusion that can be drawn regarding abrasion rates in the American Arctic is that the results of this investigation as expressed in terms of ice velocity and ice thickness should be regarded as a conservative estimate. The reason for this is that Baltic Sea ice is generally harder and stronger than Arctic sea ice, at least as far as first year ice is concerned. More precise estimates with quantified reduction of ice abrasion due to higher sea water salinity than in the Baltic, and consequently weaker ice, should only be made after additional field abrasion studies which include areas with higher water salinity than the Baltic.

The concrete material is about the same in all the lighthouses. They have been designed to meet the Swedish concrete code for structures in a marine environment. The only intended differences in concrete quality between the lighthouses are those caused by revision of the standard code specifications. See the sub-report Technical Description of the Lighthouses, Volume II.

Consequently, the results from this study are applicable only to structures made of concrete with at least the same ice abrasion resistance as that of the lighthouses. The concrete is briefly described as follows

Cement: Swedish Portland cement
Coarse aggregate: Naturally available granite with rounded shape
Fine aggregate: Naturally available sand
Additives: air-entraining agent (only after 1965)
Cement content: 300-400 kg/m^3
Specified cube strength: 40 MPa

The material investigation, that has been part of this study, shows that actual strength and cement content has been well above the specified values for the 4 investigated lighthouses.

There is a tendency in Sweden for concrete strength, cement content and air pore volume to be higher in the newer marine structures than in the older ones. However, this fact is not reflected in any observed higher resistance against ice abrasion, taking into account the probable influence of ice velocity and ice thickness.

Thus, one important conclusion is that ice velocity and ice thickness are much more important factors governing abrasion rate than the concrete quality, provided always that the concrete is of at least the normal standard for marine structures.

Whether or not this conclusion can be extrapolated so that abrasion rate found in this investigation as a function of ice velocity and ice thickness can be regarded as reasonably valid also for high strength lightweight aggregate concretes which are of interest for Arctic applications, is a matter for continued studies.

3.2 Recommendations for future studies

It is clear from this investigation that moving ice causes significant damage to offshore concrete structures which should be considered in the design work. As the investigation is basically a systematic mapping of the ice impact on a number of existing structures complemented by the evaluation of ice statistics and testing of the concrete quality, there are some obvious limitations with respect to the conclusions that can be drawn. The main limitations are:

1. The true mechanism of the ice impact on a concrete surface is not directly revealed by the investigation. The abrasion rate is given as total abrasion divided by number of years after installation. It would be of great value for a definitive understanding of how ice affects a concrete structure to know the abrasion that occurs during each specific winter season and to relate the abrasion to the specific ice condition.

2. The concrete quality is about the same in the case of all the lighthouses. For Arctic structures, it is of special interest to be able to predict the abrasion rate in lightweight aggregate concrete structures. However, this cannot be done directly on the basis of the current investigation. This question is coupled with considerations regarding the true mechanism of the ice impact.

3. Only structures in the Baltic are covered. In the Arctic, where the salinity is higher, the ice is not so hard and strong and, consequently, less abrasion can be foreseen provided that other parameters are the same. Whether or not this conclusion is accurate cannot be judged on the basis of this investigation only.

Items 1 and 2 above, can be clarified by continued field investigations in the Baltic, which is very convenient as the test sites are easily accessible, while for item 3 field studies have to be carried out in Arctic areas.

The main recommendation is therefore to follow up this investigation with continued studies of the ice impact on some of the most exposed lighthouses. Some of them, for instance the Sydostbrotten lighthouse, will have to be repaired before the ice abrasion has reached an excessively advanced stage. It will thus be possible to combine repair with field testing of the abrasion resistance of different concretes.

Prestudies have been made of the feasibility of installing precast lightweight aggregate panels around the circumference of the caisson wall of the Sydostbrotten lighthouse. These panels should be attached to the caisson structure in such a way that they will not come loose by the action of ice impact. Fig. 3.2 shows a layout of the system.

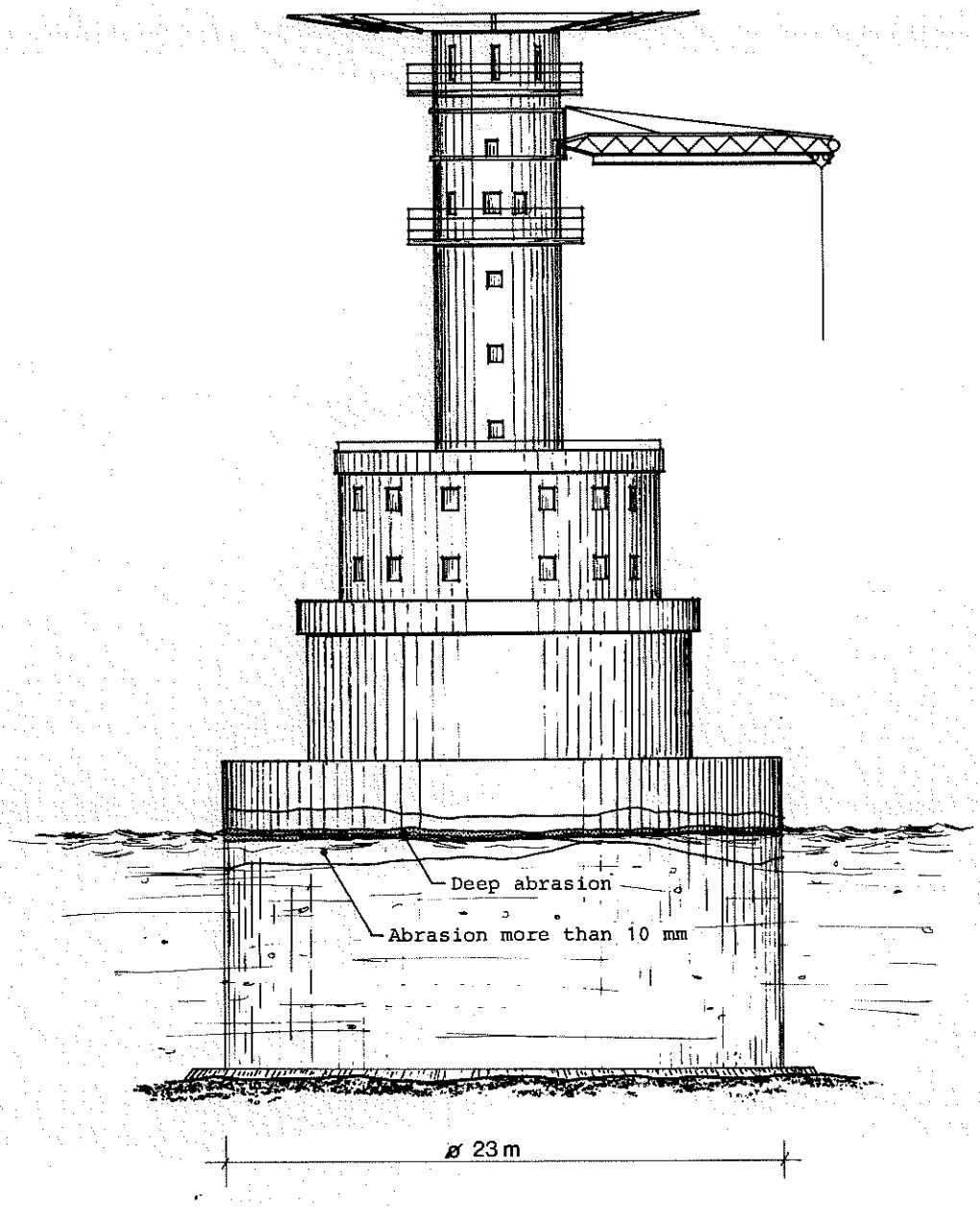

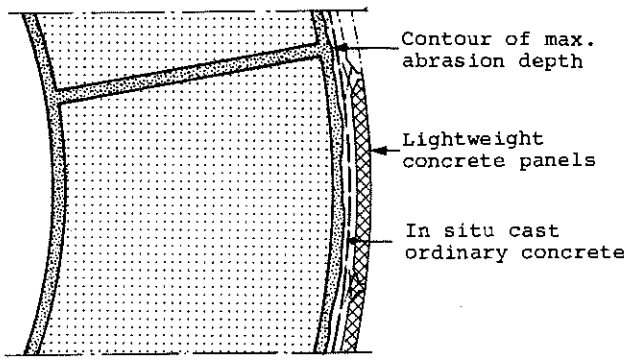

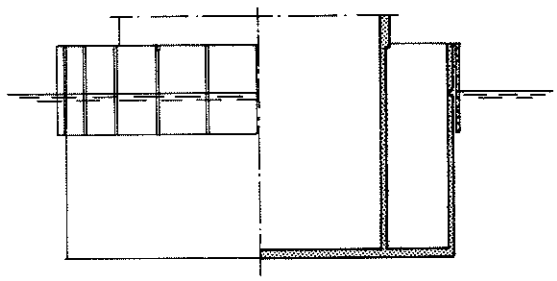

Fig. 3:2 The Sydostbrotten lighthouse equipped with precast lightweight aggregate concrete panels.

The investigation should include the following activities

1. Installation of precast concrete panels at the Sydostbrotten lighthouse.

   The circumference of the caisson is about 70 m, and it is shown in the current study that a great part of the circumference is severely affected by ice abrasion. Therefore, panels of certain different concrete qualities, including both lightweight aggregate concretes and ordinary concrete, can be used.

2. Detailed evaluation of ice statistics.

   There are more ice statistics available at SMHI than have been possible to consider in the current study. Based on the results of the current study, deep penetration of available statistics for a few selected lighthouses should be done. Then, more accurate information regarding v, s and t will be gained including also ice drift direction.

3. Detailed study of the ice behaviour at the Sydostbrotten lighthouse.

   This should be done both by cameras that are permanently installed and automatically started and by engineers visiting the lighthouse on occasions with severe or otherwise interesting ice behaviour.

4. Description of ice strength.

   Several times during the winter season, the ice strength and other ice parameters that could affect its ability to have an abrasive effect on the concrete caisson should be tested or estimated by ice experts.

5. Inspection of possible erosion and other visible results of the ice impact on the concrete surface near and below the water line.

   This will include only one or two days' work at the site in the early summer.

Items 3-5 above should be repeated every year. To come to a useful result of the investigation, 3 winter seasons should be included. Whether

or not the program shall be continued after 3 years should be decided based on the result from 3 years.

The reports from the investigation should be issued as follows:

Report 1

- Detailed description of the panels including material test results.
- Detailed description of all work at the lighthouse including installation of the panels and instrumentation.

Report 2

- Evaluation of detailed ice statistics at the Sydostbrotten lighthouse and at some other lighthouses.
- Revised analysis of the correlation between ice characteristics and observed abrasion. This will be a valuable complement to the current study.

Reports 3-5

- Yearly reports after every winter season.

Report 6

- Final conclusions and summary.

OG 306d-003b
JEJ/MIA/GA
1984-08-30

4. REFERENCES

ADAMS, N., et al. (1982): "BP think-tank takes a fresh look at ice forces". Extracts from a paper to the Second Symposium on Applied Glaciology, Hanover, New Hampshire, USA. Offshore Engineer, October 1982.

APOA Project No. 57 (1973): "Adfreeze Study". Acres Consulting Services, Calgary.

APOA Project No. 85 (1975): "Preliminary Assessment of the Adhesion Shear Strength of Ice -Steel and Ice - Frozen Sand Bands". Arctec Canada Ltd., Montreal, Quebec.

ASSUR, A. (1971): "Forces in moving ice fields". POAC 1971, Vol. 1, pp. 112-118.

BERGSTRÖM, S.G. (1955): "Frysförsök med cementbruk". Swedish Cement and Concrete Research Institute, Message. No. 32, Stockholm, 1955.

BLENKARN, K.A. (1970) "Measurements and analysis of ice forces on Cook inlet structures". OTC 1261.

BÄUMEL, A. & ENGELL, H.J. (1959): "Korrosion von Stahl in Beton". Archiv für das Eisenhüttenwesen, 30(1959): 7, pp. 417-428.

CEMBUREAU (1978): "Use of concrete in aggressive environments". Cembureau recommendation, 1st edition. Paris, 1978.

CEMENTA AB (1983): "Betongkonstruktioners beständighet (Durability of concrete structures)". Brochure, Cementa AB, Danderyd, Sweden.

CHATTERJI, S. & JEFFERY, J.W. (1963): "A new hypothesis of sulphate expansion". Magazine of Concrete Research, 1963:44.

CLEAR, K.C. (1974): "Time to corrosion of reinforcing steel in concrete slabs". Transportation Research Record 500, 1974.

CORDON, W.A. (1966): "Freezing and thawing of concrete - Mechanisms and control". American Concrete Institute, Monograph No. 3. Detroit, 1966.

COX, G.F. & WEEKS, W.F. (1974): " Salinity variation in sea ice". Journal of Glaciology, Vol. 13, No. 67, pp. 109-20.

CROASDALE, K.R. (1977): "Ice engineering for offshore petroleum exploration in Canada". POAC 1977, Vol. 1.

DEUTCHER AUSSCHUSS FÜR STAHLBETON, H. 170 (1965): "Beobachtung an alten Stahlbetonbauteilen hinsichtlich Carbonatisierung des Betons und Rustbildung an der Bewehrung". G. Rehm und H.L. Moll. "Undersuchnung über das Fortschreiben der Carbonatisierung and Betonbauwerken". H.-J. Kleinschmidt. "Tiefe der carbonatisierten Schicht alter Betonbauten Untersuchnungen an Betonproben". Forschungsinstitut für Hochofenschlacke, Reinhausen und Laboratorium der Westfälishen Zementindustrie, Beckum, Berlin 1965, 59 p.

DIAMOND, S. (1975-76): "A review of alkali-silica reaction and expansion mechanisms, 1. Alkalies in cements and in concrete pore solutions." Cement and Concrete Research 5 (1975):4. "2. Reactive aggregates". Cement and Concrete Research 6 (1976):4.

DICKINS, D.F. & WETZEL, V.F. (1981): "Multi-Year Ridge Study Queen Elizabeth Islands". POAC 1981, Vol 2.

DYKINS, J.E. (1967): "Tensile properties of sea ice grown in a confined system". In Physics of Snow and Ice, Vol. 1, Part 1, pp. 523-537, Institute of Low Temperature Science, Hokkaide Univ.

DYKINS, J.E. (1970): "Ice engineering: tensile properties of sea ice grown in a confined system". Naval Civil Engr. Lab. Tech. Rep. R689, 56 pp., Port Hueneme, Calif.

DYKINS, J.E. (1971): "Ice engineering: material properties of saline ice for a limited range of conditions". Naval Civil Engr. Lab. Tech. Rep. R720, 95 pp., Port Hueneme, Calif.

EIDE, L.I. & MARTIN, S. (1975): "The formation of brine drainage features in young sea ice". Journal of Glaciology, Vol. 14, No. 70, pp. 137-154.

ENGELBREKTSON, A. (1977): "Dynamic Ice Loads on a Lighthouse". POAC 1977, Vol. 2.

ENGELBREKTSON, A. (1983): "Observations of a Resonance Vibrating Lighthouse Structure in Moving Ice". POAC 1983, Vol. 2.

ENGELBREKTSON, A. (1983): "Ice Force Design of Offshore Structures". Paper presented at the international conference "Offshore Göteborg 83".

FAGERLUND, G. (1983): "Pozzolaner i betong". Cementa 1983:2.

FORSSBLAD, L. (1972): "Kvalitetskrav, provnings-förfarande och arbetsmetoder vid betonggolvarbeten". Nordisk Betong 1972:3.

FRANKENSTEIN, G.E. (1967): "Ring tensile strength studies of ice". U.S. Army, Cold Regions Research and Engineering Laboratory (CRREL) Rep. 172, 6 pp.

FREDERKING, R. & GOLD, L.W. (1975): "Experimental Study of Edge Loading on Ice Plates ". Can. Geotech. J. 12.456.

GJØRV, O.E. (1968): "Durability of Reinforced Concrete Wharfves in Norwegian Harbours". The Norwegian Committee on Concrete in Seawater, Ingeniørforlaget A/S, Oslo 1968.

HAGERMAN, T. & ROOSAAR, H. (1955): "Kismineralens skadeinverkan på betong". Betong 1955:2.

HIGHWAY RESEARCH BOARD (1964): "Symposium on alcali-carbonate rock reactions". Highway Research Board, Number 45, Washington D.C., 1964.

HOLLAND, T.C. (1983): "Abrasion - Erosion Update". Concrete Structures, Repair and Rehabilitation, Vol. C-83-1, Aug. 1983. U.S. Army Engineer Waterways Experiment Station, Vicksburg, Miss., USA.

HORJEN, I. (1980): "A Survey of the Mechanical Properties of Sea Ice". Marine Structures and Ships in Ice, A Joint Norwegian Research Project, Report No. 80-01.

KAN, T.K., et al. (1973) "Sonar Mapping of the Underside of Pack Ice". AIDJEX Bulletin No. 21, Seattle, WA., pp. 155-169.

KEINONEN, A. (1977): "Measurements of physical characteristics of ridges on April 14 and 15, 1977". Styrelsen för Vintersjöfartsforskning, Research report no. 22, 1977, Helsinki.

KEINONEN, A. (1978): "Presentation of sea ice ridges in general and physical characteristics of Baltic ridges for ship resistance calculations". Styrelsen för Vintersjöfartsforskning, Research report no. 24, 1978, Helsinki.

KENNEDY, H.L. & PRIOR, M.E. (1955): "Abrasion resistance. Significance of tests and properties of concrete and concrete aggregates". ASTM Special Technical Publication No. 169. Philadelphia, Pa., 1955.

KIVISILD, H.R. (1976): "Offshore structures in Arctic ice". BOSS 1976.

KOVACS, A., (1971): "On Pressured Sea Ice". Sea Ice - Proceeding of an International Conference, Reykjavik, Iceland, pp. 276-295.

KOVACS, A., WEEKS, W.F., ACKLEY, S. & HIBLER III, W.D. (1973): "Structure of a multi-year pressure ridge". Arctic, Vol. 26, No. 1, pp. 22-31.

LANGLEBEN, M.P. & POUNDER, E.R. (1963): "Elastic parameters of sea ice" in "Ice and snow - Processes, properties, and applications" (W.E. Kingery, Ed.). Cambridge, Mass; MIT Press, pp. 69-78.

LAVROV, V.V. (1969): "Deformation and Strength of Ice", Arctic and Antarctic Scientific Research Institute (Leningrad 1969) Israel Program for Scientific Translations, Jerusalem, 1971.

LOCHER, F.W. (1966): "Zur Frage des Sulfatwiderstands von Hüttenzementen". Zement- Kalk-Gips 19 (1966):9.

LOCHER, F.W. (1968): "Influence of chloride and hydro-carbonate on the sulphate attack". Proc. Fifth International Symposium on the Chemistry of Cement. Part III, Tokyo 1968.

MATHISEN, J.-P. (1981): "Ice and other Environmental Data from the Arctic". Marine Structures and Ships in Ice, A Joint Norwegian Research Project, Reports Nos 81-01/1-2.

MEYER, A., WIERIG, H.J. & HAUSMANN, K. (1967): "Karbonatisierung von Schwerbeton". Deutsche Ausschuss für Stahlbeton, Heft 182. W. Ernst & Sohn, Berlin 1967.

MICHEL, B. (1970): "Ice pressure on engineering structures". CRREL, Monograph III-BIb, 1970.

MICHEL, B. (1978): "Ice Mechanics". Les Presses de l'Université Laval, Québec 1978.

MICHEL, B. & TOUSSAINT, N. (1976): "Mechanisms and Theory of Indentation of Ice Plates". Symposium on Applied Glaciology, Cambridge, England, 1976.

MÄÄTTÄNEN, M. (1977): "Stability of self-exited ice-induced structural vibrations". POAC 1977, Vol. 2.

NÜRNBERG, H.W., WOLFF, G., HIRCH, D. & LUDWIG, U. (1973-74): "Die physikalish-chemischen Aspekte der Alkali-Kiseläure-Reaktion und ihre Bedeutung für die Treiberscheinungen in Beton". Sprechsaal für Keramik, Glas, Baustoffe, Sonderdruck aus (1973):24, (1974):3 und (1974):5.

OTTOSON, G. & SAHLMAN, L. (1975): "Provningsmetoder för betonggolv. Avnötning. Vidhäftning". Statens Provningsanstalt. Teknisk Rapport, pp. 66-107. Stockholm 1975.

PAIGE, R.A. & LEE, C.W. (1967): "Preliminary Studies of Sea Ice in McMurdo Sound, Antarctica during "Deep Freeze 65". "Journal of Glaciology, Vol. 6, No. 46.

PALOSUO, E. (1975): "The formation and structure of ice ridges in the Baltic". Styrelsen för Vintersjöfartsforskning, Research report No. 12, 1975, Helsinki.

PAULSSON, C. (1969): "Avnötning på vakuumbehandlat betonggolv". Cement & Betong 1969:3.

PAULSSON, C. & SAMUELSSON, P. (1968): "Avnötning på betonggolv". Cement & Betong 1968:4.

PEYTON, H.R. (1966): "Sea ice strength". Geophysical Institute, Univ. Alaska, Report UAG-182, 187 pp.

POUNDER, E.R. (1965): "The Physics of Ice", Pergamon Press, London.

POWERS, T.C., COPELAND, L.E., HAYES, J.C. & MANN, H.M. (1954): "Permeability of portland cement paste". Journal of the American Concrete Institute, 51(1954), pp. 285-298.

POWERS, T.C. & HELMUTH, R.A. (1953): "Theory of volume changes in hardened portland cement paste during freezing". Proc. of the Highway Research Board, 32 (1953), pp. 285-297.

PRESSLER, E.E., BRUNAUER, S., KANTRO, D.L. & WEISE, C.H. (1961): "Determination of the free calcium hydroxide contents of hydrated portland cements and calcium silicates". Anal. Chem 33 (1961), pp. 877-882.

REEH, N. (1972): "Isens fysiske egenskaber". Danmarks tekniske Højskole.

ROOSAAR, H. & VESSBY, E. (1962): "Betongskador orsakade av kiselmineral i ballast". Nordisk Betong 1962:3.

ROSENQVIST, I. (1959): "Hydrauliske gradienter og saltvandring i betong". Nordisk Betong, Stockholm, 3(1959), pp. 220-225.

ROSENQVIST, I.T. (1961): "Korrosjon av armeringsstål i betong". Teknisk Ukeblad, Oslo (1961), pp. 793-795.

SACKINGER, W.M. (1977): "Shear Strength of the Adfreeze Bond of Sea Ice to Structures". POAC 1977, Vol. 2.

SCHWARTZ, J. (1971): "The presure of floating ice-fields on piles". IAHR Ice Symposium 1970 in Reykjavik, Iceland.

SCHWARZ ET AL. (1974): "Effect of ice thickness on ice forces". OTC 2048.

SCHWARZACHER, W. (1950): "Sea ice studies in the Arctic Ocean". Journal of Geophysical Research, Vol. 64, pp. 2357-2367.

SHALON, R. & RAPHAEL, M. (1959): "Influence of seawater on corrosion of reinforcement". Proc. of the American Concrete Institute, 55(1959), pp. 1251-1268.

SHUMSKII, P.A. (1964): "Principles of Structural Glaciology". Dover Publications Inc., New York.

SISODIYA, R.G. & VAUDREY, K.D. (1981): "Beaufort Sea First-Year Ice Features Survey - 1979". POAC 1981, Vol. 2.

SMHI, Swedish Meteorological and Hydrological Institute, Norrköping, Sweden & Institute of Marine Research, Helsinki, Finland (1982): "Climatological Ice Atlas for the Baltic Sea, Kattegat, Skagerrak and Lake Vänern (1963-1979)".

SPRINGENSCHMID, R. & SOMMER, H. (1971): "Untersuchungen über die Verschleissfestigkeit von Strassen-beton bei Spikereifen - Verkehr". Strasse und Autobahn 1971:4.

STEINOUR, H. H. (1964): " Influence of the cement on the corrosion. Behaviour of steel in concrete". Portland Cement Association, Research and Development Laboratories, Research Department, Bulletin 168, May 1964, 14 p.

SVENSK BYGGTJÄNST (The Swedish Building Centre) (1980): "Betonghandboken, Material (Concrete Handbook, Material)", 1980.

SWENSON, E.G. (1972): "Interaction of concrete aggregates and portland cement - Situation in Canada". Engineering Journal. Engineering Institute of Canada, 55 (1972):5.

TABATA, T., FUJINO, K. & AOTA, M. (1966): "The flexural strength of sea ice in-situ". Proceedings of conference, Institute of Low Temperature Sciences, Hokkaido University, Aug. 1966.

TABATA, T. ET AL. (1967): "Studies of the mechanical properties of sea ice XI". Hokkaido University. Sapporo.

TRANSESHE, N.A. (1928): "The ice cover of the Arctic Sea with a genetic classification of sea ice". Publ. of Polar Research, A.G.S., Special Publ., No. 7, pp. 91-123.

TRANSPORTATION RESEARCH BOARD (1974): "Cement-aggregate reactions". Transportation Research Record 525, Transportation Research Board, Washington D.C., 1974.

U.S. BUREAU OF RECLAMATION (1955): "Investigation into the effect of water-cement ratio on the freezing-thawing resistance of non-air and air-entrained concrete". Concrete Laboratory Report No. C-810, Denver, 1955.

VAAGE, B., VERLO, P.O. & FOKK, T. (1979): "Resistance in Ice". Marine Structures and Ships in Ice, A Joint Norwegian Research Project, Report No. 79-01.

VAUDREY, K.D. (1977): "Determination of Mechanical Sea Ice Properties by large-scale Field Beam Experiments". POAC 1977, Vol. 1, pp. 529-543.

VAUDREY, K.D. (1977): "Ice Engineering - Study of related Properties of Floating Sea-ice Sheets and Summary of Elastic and Viscoelastic Analyses". Technical Report, Civil Engineering Laboratory, Port Hueneme, California.

VEREIN DEUTSCHER ZEMENTVERKE (1973): "Vorbeugende Massnahmen gegen Alkalireaktion im Beton". Schriftenreihe der Zementindustrie, Heft 40/1973. Beton-Verlag GmbH, Düsseldorf 1973.

WARRIS, B. (1964): "The influence of air-entrainment on the frost-resistance of concrete. Part B. Hypothesis and freezing experiments". Swedish Cement and Concrete Research Institute. Document No. 36, Stockholm 1964, 130 pp.

WEEKS, W.F. & ASSUR, A. (1967): "The mechanical Properties of Sea Ice". U.S. Army, Cold Regions Research and Engineering Laboratory (CRREL) II-C3, Hannover 1967.

WOODS, H. (1968): "Durability of concrete construction". Monograph No. 4. American Concrete Institute. Detroit 1968.

APPENDIX I

SEA ICE MECHANICS

1. Introduction

When discussing the impact of ice on offshore structures it is of great importance not only to concentrate on the structure itself in terms of stability but also to gain an understanding of the interaction between the ice and the construction material and thus the basic mechanical behaviour of ice as a material.

In the following, the formation and mechanical properties of sea ice and pressure ridges will be discussed. In addition, comparisons will be made between the ice in the Arctic region and the ice affecting the Swedish offshore lighthouses. As regards ice conditions in the Swedish waters, the discussion will be focused on the conditions in the Gulf of Bothnia as being the most representative in comparison with the Arctic region. The presentation is based on literature studies and is intended to be a general review of the state-of-the-art of sea ice mechanics.

2. Formation of Sea Ice and Pressure Ridges

2.1 Phase Equilibrium in Sea Ice

The composition of sea water, from which the ice originates, is remarkably uniform in the oceans even if the total concentration of salts varies from one site to an other and decreases appreciably in the deltas of large rivers. The total amount of solids, in parts per thousand, is usually defined as the salinity of sea water. A salinity of 34.5 o/oo is a reasonably good average and is often taken as a standard figure. The percentage of the various salts in sea water is as follows (Michel (1978)):

NaCl	$MgCl_2$	Na_2SO_4	$CaCl_2$	KCl	$NaHCO_3$	Other	Total
68.10	14.44	11.37	3.19	1.91	0.55	0.44	100

Percentage composition of salt in sea water

As the various salts are almost completely ionized in solution, the composition of sea water is best described in terms of ionic concentration (Svensk Byggtjänst (1980)):

Cl^-	Na^+	SO_4^{2-}	Mg^{2+}	Ca^{2+}	K^+
20.00	11.10	2.81	1.41	0.48	0.40

Ion concentration in sea water in kg/m^3

The major difference between sea ice and fresh water ice is the amount of salts, in the form of concentrated brine pockets, that are squeezed within the ice structure. Therefore, the first prerequisite for the study of the structure of sea ice is a knowledge of the phase diagram. Such a diagram is shown on Fig. I:1. It gives the relative volumes of ice, brine and solid salts that will be in equilibrium at a given temperature.

Because of the salt content in sea water, the freezing point will be depressed below zero °C as shown on Fig. I:1. For "standard" sea water, this temperature of freezing is -1.8°C. For any temperature, the diagram gives the amount of brine that will coexist in equilibrium with the ice.

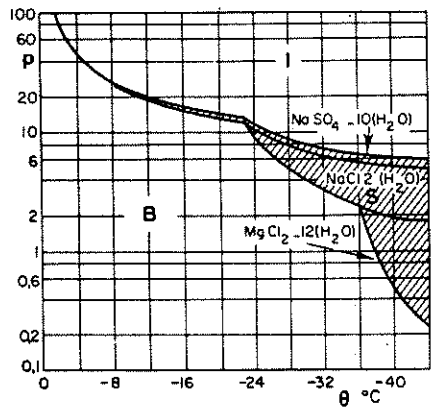

Fig. I:1 Phase diagram in the solidification of sea water showing the percentage p in weight of the various phases. I = solid ice, B = brine and S = precipitated salts (Michel (1978)).

2.2 Formation of Sea Ice

Initially, if the surface is very calm and the temperature gradient small, a few crystals will appear on the supercooled layer of water at the surface to form plate ice of uniform texture. Generally, however, wind and waves will mix the water on top of the sea and the supercooling will extend to a certain water depth. Nucleation induced by crystals or surface supercooling will initiate the formation of frazil particles having the form of small discoids. As they grow and agglomerate in slush they will float to the surface and freeze to form the first layer of ice. In polar regions, small ice nuclei coming from the atmosphere are being deposited almost

continuously on the water surface to initiate frazil formation. Little or no supercooling is then observed on the top water surface.

Once this initial skim of ice is formed, the salt in sea water plays a major role in the structure of the ice formed by thermal growth and it becomes quite different from fresh water ice. One major difference is the non-uniform growth of sea ice at the ice-water boundary. The lower part of the ice layer consists of pure ice platelets with layers of trapped brine in between. Within one and the same ice crystal, the platelets coincide with the basal plane and are accurately parallel to each other. It can also be noticed that these planes are vertical or very close to the vertical.

As freezing progresses, the platelets thicken up slightly and ice bridges develop between neighbouring ones, gradually forming an almost solid structure. The brine which is trapped behind the links forms elongated cells between the platelets, which are called brine pockets. These pockets are aligned in rows separating the platelets. The brine cells shrink in size as the ice cools forming parts of long vertical cylinders with almost microscopic cross-sections. Thus, each single crystal of sea ice is composed of a stack of parallel ice plates and each plate is separated by an array of brine pockets.

2.3 Salinity Profiles in Young Sea Ice

The physical properties of sea ice depend very much on the brine content, and this parameter varies with time because of both temperature and salinity changes. The salinity of sea ice changes in two ways; by brine drainage and by brine migration.

Pounder (1965) says that brine cells have interconnections so that brine may drain slowly through the ice under the influence of gravity, at least at temperatures above -15°C. Fig. I:2 shows a sketch of the brine drainage system which was observed by Eide et al., (1975) in young sea ice. The main channel had a diameter of the order of 1 cm and the orifice at the neck decreases to a diameter of about 2-3 mm. It was found that the brine in the channels would oscillate and thus be replaced by some of the underlying sea water.

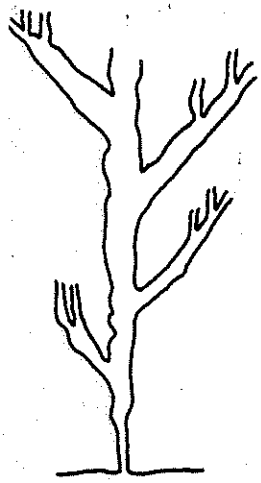

Fig. I:2 Sketch of a drain for brine in young sea ice (Eide et al (1975)).

Pounder says that brine drainage is quite rapid as ice approaches its melting point. If a block of ice is removed from contact with the sea, such as by being pushed up on to a shore, it loses salt very rapidly during the warmer months of spring and summer.

A much slower process is that of migration of the brine cells from the colder end to the warmer end of the ice sheet. Because the concentration of brine within a cell is uniform, the warmer end of it is too concentrated and will dissolve to reduce its concentration. At the colder end more ice freezes to increase the brine concentration. The net effect is to move the entire cell of brine along the temperature gradient, which is downward in a natural sea ice cover.

Both brine drainage and brine migration reduce considerably the salinity of sea ice compared to that of the surrounding sea. These processes will depend somewhat on the texture of the ice. In refrozen sea water, in snow or frazil slush and in aglomerate ice, the drainage channels cannot follow the vertical so easily and the drainage process is certainly much slower. Because of these factors, the salinity profiles in sea ice will depend very much on the ice structure and will vary considerably with time, mainly from one season to the other. An example of salinity profiles for growing sea ice of columnar structure is shown on Fig. I:3.

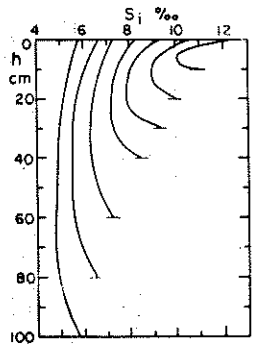

Fig. I:3 Series of schematic salinity profiles, Si, for sea ice of various thickness, h. From Weeks and Assur (1967).

2.4 Polar Ice

The Arctic ocean and part of the adjoining seas, as well as the regions surrounding the Antarctic continent are almost entirely covered the year round with polar ice which is several years of age. When there is no snow cover, the ice appears to be pale blue in colour in contrast with the greyish white of first-year ice. A polar floe is not level but is covered with gently rounded hummocks of the order of 1 m in height, spaced 30 to 40 m apart.

In the Arctic, the ice formation can be described as including the Arctic Pack, the fast ice and the drift ice (Transehe, 1928). A sketch of typical winter ice conditions in the Beaufort Sea is shown on Fig. I:4.

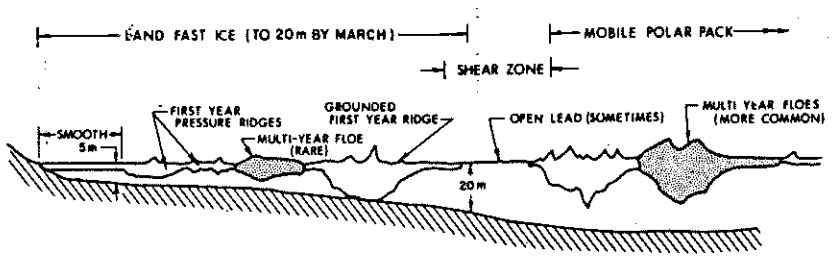

Fig. I:4 Typical winter ice conditions, Beaufort Sea (Croasdale (1977)).

The Arctic Pack floats in the centre of the Arctic ocean, covering two thirds of it. It is a permanent feature and the ice in it is progressively renewed. In July 1954, Shumskii (1964),

measured the following ice thicknesses: 10 cm of snow, 40 cm of regelation ice formed by refreezing of melt water and corresponding to four years of accumulation, 110 cm of ice having more than four years but with low salinity and finally 130 cm of sea ice having less than four years of age. The total thickness was 3 m. The approximate equilibrium limit for ice in the Arctic Pack appears to be 3-4 m (Mathisen (1981)).

The Arctic Pack turns in a clockwise direction and although the velocities depend very much on location and period of the year, a typical velocity at the periphery is of the order of 2 km/year.

The fast ice in the Arctic is the ice that forms each winter between the coasts and the Pack itself. It covers approximately 5% of the Arctic regions. It has a smooth surface interrupted by pressure ridges. Under the influence of the tides and other forces, open cracks are formed, some in contact with the grounded ice. During the summer months, fast ice is broken, melts or drifts away.

The drift ice is the multi-year ice that is not completely melted each year and that accumulates with wind and currents at particular locations which are different than the Arctic Pack.

Maximum thickness of first-year polar ice varies depending on location. In the Beaufort Sea the ice becomes 2-2.5 m thick whereas the figures for the northern and southern parts of the Bering Sea are 0.7-1.3 m and 0.3-0.7 m, respectively (Mathisen (1981)).

Multi-year polar ice attains an equilibrium thickness because the ice and snow which melt or evaporate at the top during the summer months is compensated by sea ice growth underneath during the colder periods. Because the melt water is essentially fresh and refreezes inside the brine drainage system, the salinity of polar ice is low and it is fairly strong. Salinity measurements by Cox and Weeks (1974) and Schwarzacher (1950) are shown on Fig. I:5.

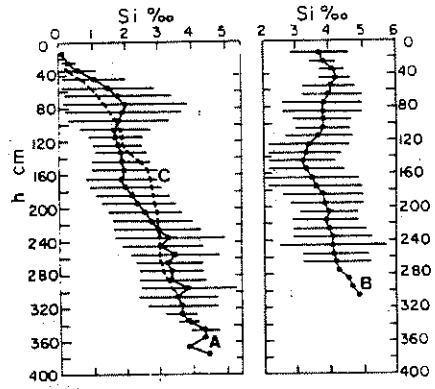

Fig. I:5. Average salinity profile in the Polar Pack. Curves A and B are the average salinities under hummocks or depressions, respectively from Cox and Weeks (1974) and C is the average given by Schwarzacher (1950). The bars denote the standard deviation of the average values.

2.5 Polar Pressure Ridges

With the exception of ice islands and icebergs, the more massive appearance of ice in the Arctic are the pressure ridges, i.e. those linear or irregular accumulations of ice caused by the crushing and shear interaction between large ice fields. The highest free floating ice ridge reported by Kovacs et al., (1973) had a sail of 12.8 m above sea level. Ridges of that size are rare and ridge sails seldom exceed 5 m. The deepest ridge keel recorded had a depth below sea level of 49 m. In the Beaufort Sea, multi-year ridges of 20 m thickness are relatively common. The build up of a ridge and the notations are shown in Fig. I:6.

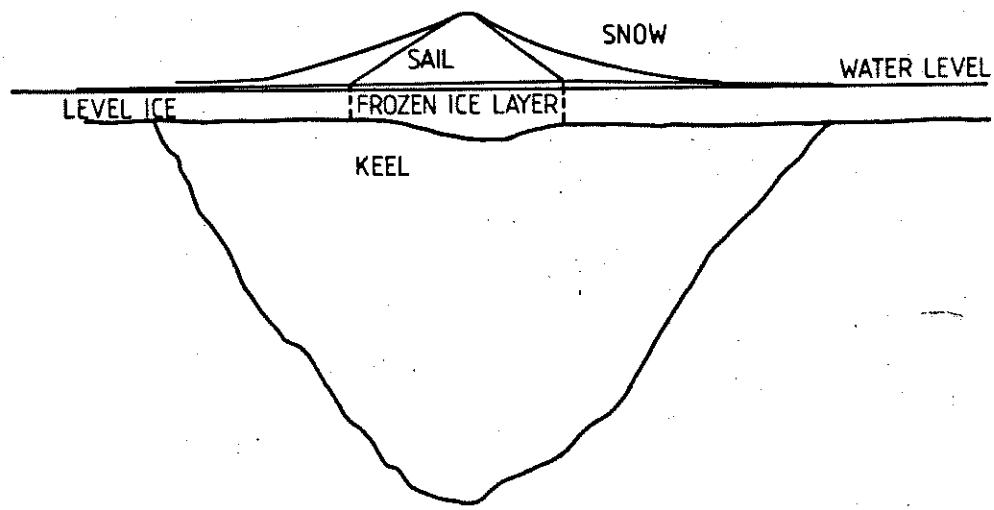

Fig. I:6 Cross-section of a pressure ridge.

The bulk properties of geometrically similar ridges may vary greatly. Ridges which have just been formed are made up of individual pieces of ice which are very poorly bounded. In a multi-year ridge, on the other hand, the melt water produced during the summer months will drain downward into the core of the ridge. Then the water will refreeze, cementing the ice blocks together into a solid, resistant mass of low salinity ice. It is thought that at least two melt seasons are required for the voids between the pieces of ice to become filled with ice.

Fig. I:7 shows sail height versus keel depth for floating first-year ridges measured in the Beaufort Sea by Sisodiya and Vaudrey (1981). The average keel depth to sail height (K/S) ratio for 17 floating ridge sections was calculated as K/S = 5.5 ± 1.2. All ridge sections with sail height greater than approx. 15 feet were grounded. This K/S value lies between the results of Kan et al. (1973), average K/S = 7.6 for five ridges, and Kovacs (1971), average K/S = 4.9 for five profiles from three separate ridges.

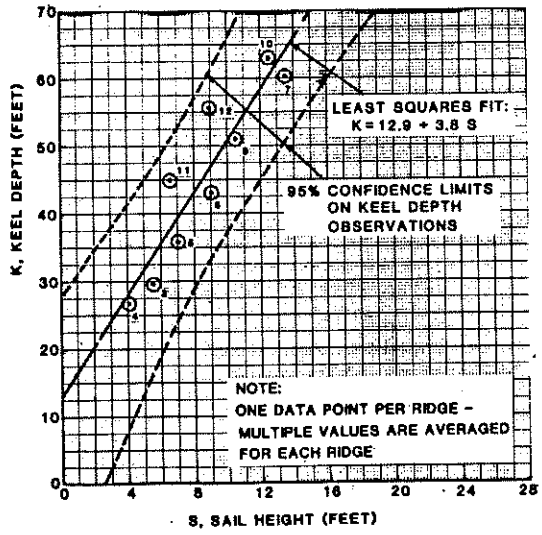

Fig. I:7 Sail height vs keel depth for floating first-year ridges (Sisodiya et al. (1981)).

For multi-year pressure ridges in the Beaufort Sea a K/S value of 3.2 has successfully been applied (See Fig. I:9).

Fig. I:8a shows two transverse and the longitudinal cross-section of a multi-year pressure ridge

that was measured in the Beaufort Sea by Kovacs et al., (1973). It had a maximum sail of 4 m above sea level and a keel of 13 m, the cross-section of which can be described as roughly semi-circular. The soundings in this ridge revealed no cavity, the mean in density being 0.90 t/m^3. There were neither wide cracks nor leads that transited the ridge.

Fig. I:8b gives the salinity and temperature profiles within the ridge. The temperatures were measured in March when the ice temperature would be expected to be close to the annual minimum.

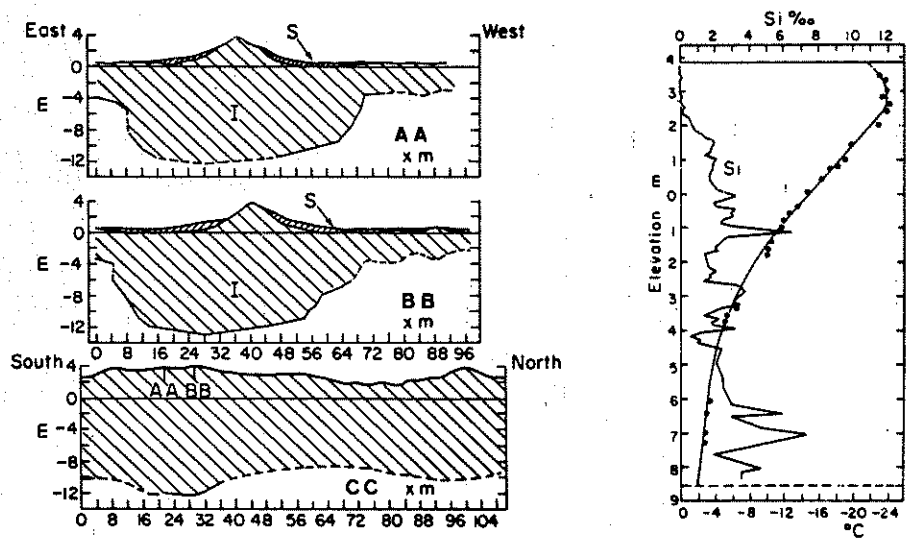

Fig. I:8a Transverse cross-sections AA and BB and longitudinal section CC of a multi-year pressure ridge in the Beaufort Sea. The limits of snow (S) and ice (I) are given.

Fig. I:8b Salinity and temperature profile of the ice in a pressure ridge. From Kovacs et al., (1973).

In studies by Dickins and Wetzel (1981) on multi-year pressure ridges in the Queen Elizabeth Islands area of the Canadian High Arctic, the average K/S value was found to be 5.6 ± 2.2. This value is considerably higher and more variable than the Beaufort Sea figure.

In the Canadian High Arctic study, a maximum keel of 37 m was observed. Underwater keel profiles were characterized by a distinct asymmetry. Average ice salinity and specific gravity was calculated at 1.7 o/oo and 0.92 t/m^3, respectively. These results mean that there could not have been any significant voids in the ridges studied, a finding supported by the visual observations of fractured sails showing total consolidation of the original blocks.

In Fig. I:9 a plot of all available multi-year ridge sail and keel dimensions is presented. The results of the Canadian High Arctic study are marked APOA Project No. 102. The other results refer to the Beaufort Sea. It is theorized that as as result of cold air and water temperatures over most of the year, the different aging processes of ridges in the Canadian High Arctic, contribute to the larger keel to sail ratios found here.

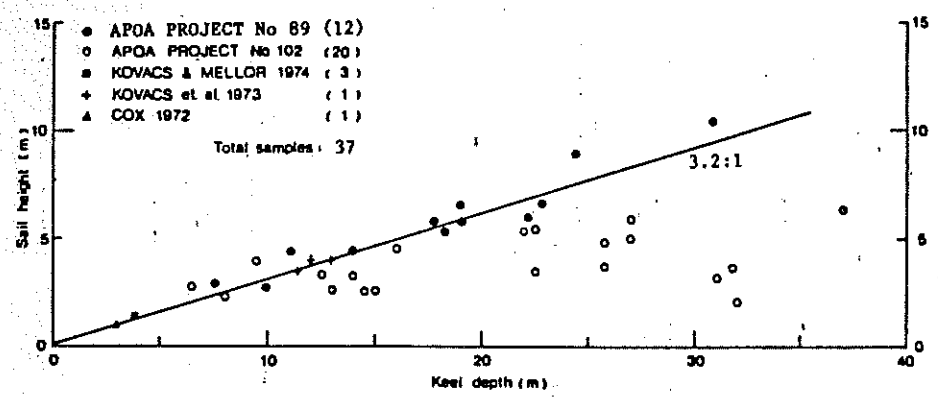

Fig. I:9 Sail height vs keel depth for multi-year pressure ridges according to all available studies.

2.6 Level Ice Features in the Gulf of Bothnia

The Bay and Sea of Bothnia, together called the Gulf of Bothnia, is the northern extension of the Baltic Sea. Both the basins are rather shallow with mean water depths of 42 and 69 m, respectively. The water salinity is low. Thus normal salinity values in the Bay and Sea of Bothnia are 2.0-3.5 o/oo and 5.0-5.5 o/oo, respectively, see Fig. I:10. The large supply of fresh water from the rivers makes the Baltic Sea more or less a brackish-water lake.

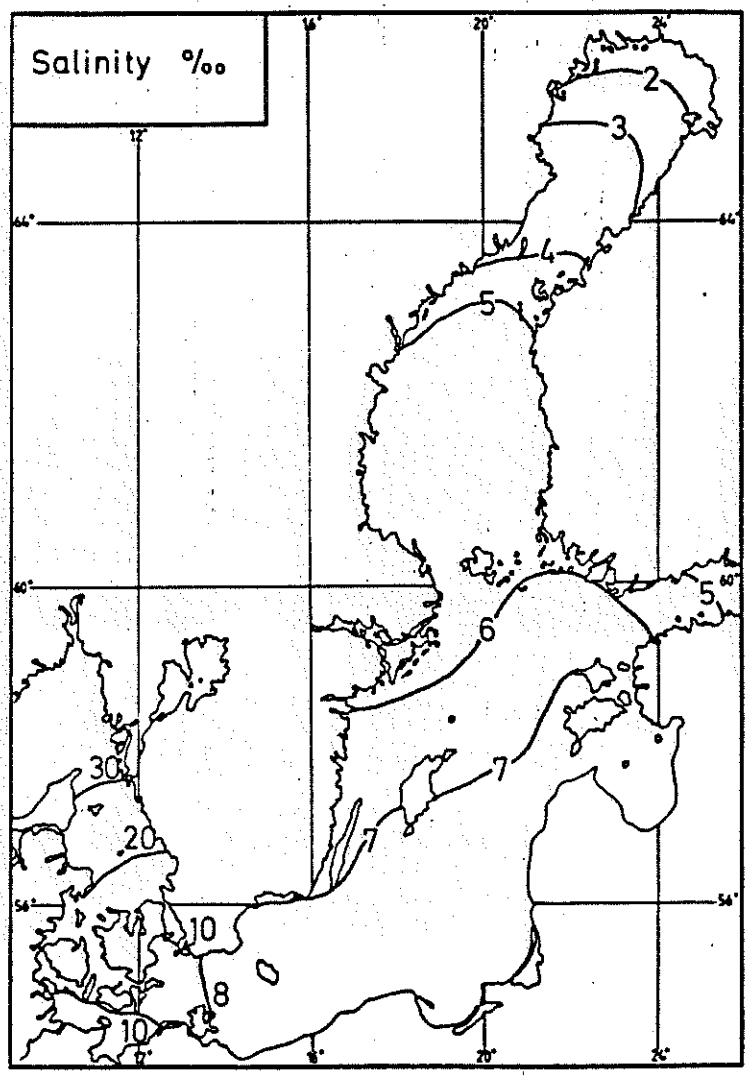

Fig. I:10 Salinity profiles in the Baltic Sea.

The ice in the Baltic does not survive the melting season and is thus first-year ice. Typical level ice thicknesses in the Bay and Sea of Bothnia are 0.5 to 0.7 m and 0.2 to 0.4 m, respectively. The corresponding estimated absolute maximum thicknesses of level sea ice are about 0.9 to 1.2 m and 0.6 to 0.9 m, respectively. At the inner skerries on the coasts the ice can be about 0.2 m thicker during normal conditions and about 0.6 m thicker during extreme winters. Level ice salinity in the Gulf of Bothnia can be expected to be approx. 0.7 o/oo (Keinonen (1978)).

The boundary between fast ice and pack ice is of considerable practical importance. The pack ice, being composed of separate pieces or floes, is free to respond to wind action. Strong offshore winds drive the pack ice away from the coast and leave a channel or lead of open water along the fast ice edge. Onshore winds close this channel by consolidating the pack against the fast ice.

In doing so they usually open a lead or larger channel along the edge for the fast ice on the opposite shore. In this way, westerly winds in Gulf of Bothnia favour the presence of an open lead near the Swedish coast; easterly winds on the other hand, favour a lead near the Finnish coast of the gulf. In a similar way, in the Gulf of Finland, southerly winds tend to concentrate the ice against the Finnish coast and to favour a lead along or near the southern shore with northerly winds having the opposite effect.

2.7 Pressure Ridges in the Gulf of Bothnia

2.7.1 General

The ridges in the Gulf of Bothnia do not survive the melting season and are thus first-year ridges. The age of the ridges can be up to six months. The proportion of ice pushed above and below the water level is determined approximately by the balanced flotation of ice. This generally means that about one eighth of the ice is pushed above the water level, thus forming the sail. The rest of the ice forms the keel below the water level.

A brief description is given below of the structure of pressure ridges in the Gulf of Bothnia. This kind of description is, however, only an approximation since the data on which it is based is limited.

The number of pressure ridges has been studied from icebreakers. During the winter of 1975-76, an average of 1.25 ridges/km were observed along a 3 600 km icebreaker route. In this context consideration was only given to ridges with keel depths exceeding about 1.5 m.

The maximum ridge keel depth and total thickness reported are 28 m and 31.5 m, respectively. Observations indicate that the mean total thickness of pressure ridges in this region is about 4 m.

2.7.2 The Sail

The structure of the sail of a pressure ridge can be summarized as follows:

- loose ice blocks with a thickness of normally 0.2 to 0.4 m and maximum length 3 to 5 times the thickness (Keinonen (1977, 1978))
- slope angle (measured from the horizontal), about 24 degrees as an average (Keinonen 1978))
- porosity about 35 to 45%
- density about 0.87 t/m^3 as an average. The topmost ice least dense (Keinonen 1977, 1978))
- the temperature increases almost linearly with increasing depth until the freezing temperature of the sea water is reached just below the frozen ice layer below the sail.
- salinity approx. 0.5 o/oo as an average (Keinonen (1978)).

2.7.3 The Frozen Ice Layer

The features of the frozen ice layer just below the sail of a pressure ridge are briefly mentioned below:

- the thickness of the frozen ice layer is greater than that of the surrounding level ice. The average additional thickness is in the order of 50-72% of the sail ice block thickness (Keinonen (1978)).
- ice density is approximately the same as that of the surrounding level ice, i.e. about 0.92 t/m^3.
- the most saline ice in the ridge is in the topmost part of the frozen ice layer. The salinity is approx. 1.4 o/oo as an average (Keinonen (1978)).

2.7.4 The Keel

The structure of the keel of a pressure ridge can be summarized as follows:

- loose ice blocks of the same thickness, size, shape, density and porosity as in the sail

- slope angle (measured from the horizontal) up to 60 degrees (Palosuo (1975))

- ice blocks rounded, deteriorated; strength decreasing downwards

- the amount of slush is significant

3. Mechanical Properties of Sea Ice

3.1 Introduction

The ice strength is found to be influenced by the following parameters:

- Grain structure
- Porosity
- Temperature
- Strain rate
- Size of test specimen

3.2 Grain Structure

The ice is built up of grains or crystals, and as a result of this, ice is not an isotropic material. According to Reeh (1972), ice crystals are nearly twice as strong when loaded parallel to the growth direction as they are when loaded at right angles to the growth direction. When ice is formed on a water surface, growth conditions are such that they favour ice crystals with a vertical growth direction. As a consequence of this, the resulting ice sheet will be weaker for loads in the plane of the sheet than for loads at right angles to the sheet. In addition, ice strength decreases with increasing crystal size. Crystal sizes generally increase as the ice sheet grows thicker.

3.3 Porosity and Temperature

The porosity is the sum of the relative volume of brine (V_b) and air (V_a). The air volume is often much smaller than the brine volume and the formulas for ice strength and moduli mostly take into account only the brine volume effect. When salt water freezes, the salt is rejected by the freezing water. The remaining water becomes increasingly saline as more water freezes. The final volume of water is too salty to freeze, and is enclosed in pores in the ice.

The effect of porosity on ice strength is directly related to the reduction of cross-sectional area caused by the pores. Ice frozen from salt water usually contains more pores than fresh water ice, and is consequently weaker. It is common for new salt-water ice to have a brine volume of 30 o/oo. On the other hand, old sea ice (multi-year ice) loses much of its brine content, see Chapter 2.4. Multi-year sea ice may therefore have a strength approaching that of fresh water ice. When ice slabs are heaped up into ridges, the air gaps between the slabs will give a relatively high (average) porosity. According to Kivisild (1976), it may be as high as 50%. According to Reeh, the ice strength seems to approach a constant value at high values of porosity.

The ice strength and moduli increase with decreasing ice temperature.

Table I:1 shows the brine volume as a function of ice temperature according to Assur (1971). The brine volume given in Table I:1 is valid for ice with a salinity of 1 o/oo, but the brine volume for any salinity S can be obtained by multiplying the values in the table by S (in o/oo).

Volume of Brine (‰)

°C	0	.1	.2	.3	.4	.5	.6	.7	.8	.9
−0	—	500.9	250.5	167.1	125.4	100.3	83.66	71.74	62.08	55.85
−1	50.28	45.77	41.87	38.60	35.77	33.29	31.07	29.06	27.23	25.56
−2	24.0	22.8	21.8	20.9	20.1	19.3	18.5	17.9	17.3	16.7
−3	16.2	15.7	15.2	14.8	14.4	14.0	13.6	13.3	13.0	12.7
−4	12.4	12.1	11.8	11.6	11.4	11.2	11.0	10.8	10.6	10.4
−5	10.2	10.0	9.81	9.64	9.48	9.32	9.16	9.01	8.87	8.73
−6	8.60	8.48	8.36	8.25	8.14	8.03	7.92	7.82	7.72	7.62
−7	7.52	7.43	7.34	7.25	7.16	7.07	6.99	6.91	6.83	6.75
−8	6.67	6.60	6.53	6.46	6.39	6.32	6.26	6.20	6.14	6.08
−9	6.02	5.97	5.92	5.87	5.82	5.77	5.72	5.67	5.62	5.57
−10	5.53	5.49	5.45	5.41	5.37	5.33	5.29	5.26	5.22	5.18
−11	5.15	5.12	5.08	5.05	5.01	4.98	4.95	4.92	4.88	4.85
−12	4.82	4.79	4.76	4.74	4.71	4.68	4.66	4.63	4.61	4.58
−13	4.56	4.54	4.51	4.49	4.46	4.44	4.42	4.40	4.37	4.35
−14	4.33	4.31	4.29	4.27	4.25	4.23	4.21	4.19	4.17	4.15
−15	4.13	4.11	4.09	4.08	4.06	4.04	4.02	4.00	3.99	3.97
−16	3.95	3.93	3.92	3.90	3.89	3.87	3.85	3.84	3.82	3.81
−17	3.79	3.78	3.76	3.75	3.73	3.72	3.71	3.69	3.68	3.66
−18	3.65	3.64	3.62	3.61	3.59	3.58	3.57	3.55	3.54	3.52
−19	3.51	3.50	3.48	3.47	3.45	3.44	3.43	3.42	3.40	3.39
−20	3.38	3.37	3.36	3.34	3.33	3.32	3.31	3.30	3.28	3.27
−21	3.26	3.25	3.24	3.22	3.21	3.20	3.19	3.18	3.16	3.15
−22	3.14	3.13	3.12	3.11	3.10	3.09	3.08	3.07	3.06	3.05
−23	2.97	2.89	2.81	2.72	2.64	2.56	2.50	2.43	2.37	2.30
−24	2.24	2.19	2.14	2.08	2.03	1.98	1.94	1.89	1.85	1.80
−25	1.76	1.72	1.69	1.65	1.62	1.58	1.55	1.52	1.49	1.46
−26	1.44	1.41	1.38	1.36	1.33	1.31	1.29	1.27	1.25	1.23
−27	1.21	1.19	1.18	1.16	1.15	1.13	1.12	1.11	1.09	1.08
−28	1.07	1.06	1.05	1.04	1.03	1.02	1.01	1.00	.990	.980
−29	.970	.960	.950	.940	.930	.920	.912	.904	.897	.889
−30	.881	.875	.869	.864	.858	.852	.846	.840	.835	.829
−31	.823	.818	.813	.808	.803	.798	.793	.788	.783	.778
−32	.773	.769	.764	.760	.756	.752	.747	.743	.739	.734
−33	.730	.726	.723	.720	.716	.712	.709	.706	.702	.698
−34	.695	.692	.689	.686	.683	.680	.678	.675	.672	.669
−35	.666	.664	.661	.658	.656	.654	.651	.648	.646	.644
−36	.641	.639	.636	.634	.632	.630	.627	.625	.623	.620
−37	.618	.616	.614	.611	.609	.607	.605	.603	.600	.598
−38	.596	.594	.592	.590	.588	.585	.583	.581	.579	.577
−39	.575	.573	.571	.569	.567	.565	.563	.561	.559	.557

°C	−40°	−42°	−44°	−46°	−48°	−50°	−52°	−54°
Brine	.555	.522	.395	.242	.162	.118	.0914	.0750

Table I:1 Brine volume as a function of ice temperature according to Assur (1971).

3.4 Strain Rate

Ice can be described as a visco-elastic material. At high strain rates ice behaves as an elastic material, while at low strain rates it creeps. At a high strain rate, ice will fail after a relatively small deformation (brittle failure) while considerable deformation can take place at a low strain rate before failure occurs (ductile failure). Consequently, the strength of ice is a function of the strain rate and reaches a maximum value at a strain rate of approx. 10^{-3} s^{-1}. According to Blenkarn (1970), Croasdale (1977), Määttänen (1977), Michel (1970) and Schwarz et al. (1974), the strength is reduced in the case of higher strain rates.

Fig. I:11 presents the results of laboratory and field tests on the relationship between ice strength and strain rate. The comparison between laboratory and field test results suggests a scale effect which, if extrapolated would lead to even lower effective ice pressures on full size structures (see also Chapter 3.5).

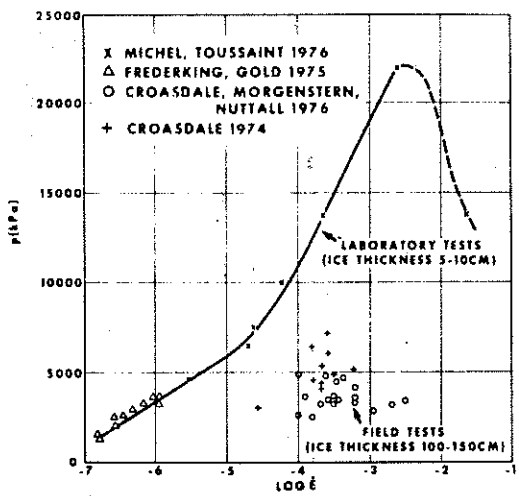

Fig. I:11 Indentation strength (p) vs strain rate ($\dot{\varepsilon}$) (Michel and Toussaint (1976))

Work by Michel and Toussaint (1976) demonstrates the phenomenon of "continuous crushing". As shown in Fig. I:12, the peak ice pressure obtained during the initial indentation with perfect contact is always much higher than the subsequent peaks. From Fig. I:12 it can also be noted that ice forces due to continuous crushing are of an oscillatory nature. According to Määttänen (1977), the reduction in ice strength with increasing strain rate is thought to contribute to this

oscillation, whic in turn may give rise to vibrations in marine structures. One example of this is the ice-induced vibrations in the Norströmsgrund lighthouse in the Bay of Bothnia, Sweden reported by Engelbrektson (1977, 1983). See also Volume II, Technical description of the lighthouses, Chapter 3.24.3.

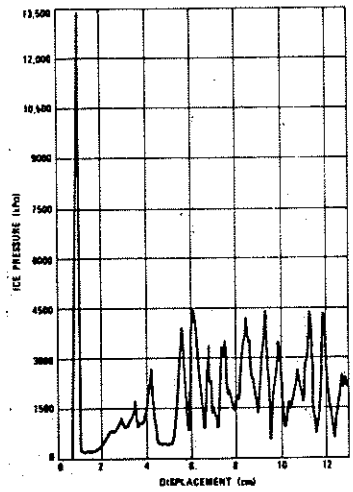

Fig. I:12 Indentation pressure vs displacement (Michel and Toussaint (1976)).

The flexural strength is shown to be constant at very low strain rates (below 2×10^{-5} s^{-1}). According to Tabata (1967), the strength increases at higher strain rates. No indication is given of what happens with the flexural strength at strain rates above 10^{-3} s^{-1} but presumably it will undergo a reduction similar to that of the compressive strength.

3.5 Scale Effect

Small test pieces of ice show higher strength than large pieces. According to Schwarz et al. (1974) the basic reason for this is that in the case of small pieces cracks must develop inside the crystals and not only at the (weaker) crystal interfaces. If the test piece is sufficiently large, cracks will develop only at the crystal interfaces, and no scale effect need be considered when the test results are used for full scale data. It is concluded that this condition is fulfilled if the diameter of the test piece is 25 times or more the diameter of a typical ice crystal.

3.6 Strength Characteristics

It is found that the strength of ice varies linearly with $\sqrt{V_b}$. For large brine volumes the strength is approximately constant.

Formulas for the tensile, compressive, flexural (bending) and shear strength are given in Table I:2. The ratio between the compressive and tensile strength appears to be approx. 7:1 whereas the horizontal tensile, flexural and shear strengths appear to be of the same magnitude.

According to Schwarz et al. (1974), laboratory tests with fine grain freshwater ice of 0°C have shown an ice crushing strength of 3.5 MPa. No scale effect is anticipated for this test. Similar tests with river ice (Schwartz (1970)) show a maximum crushing strength of 3.6 MPa at 0°C (pressure perpendicular to growth direction). In the case of brackish water ice the maximum crushing strength is 2 MPa at 0°C. According to Schwartz, the maximum crushing strength at -10°C is determined as 7 MPa for river ice and as 6 MPa for brackish water ice. Michel (1970) reports compressive ice strength of 2.8 MPa (400 psi) for fresh water ice at -5°C. According to Kivisild (1976), the compressive strength of sea ice is 4-8 MPa depending on temperature.

Adams et al. (1982) report that, in tension, sea ice fracture occurs at a stress of between 1 and 2 MPa (150-300 psi) depending on grain size, and is thought to be due to instable propagation of pre-existing microcracks. In compression, microcracks probably do not begin to propagate until a stress level about three times higher is reached, and failure follows the linking up of these distributed microcracks.

A knowledge of adfreeze strength is important to predict breakout loads when sea ice, frozen to structural surfaces, is subjected to ice movement. Several studies have been made of adfreeze including Sackinger (1977), APOA Project No. 57 (1973) and APOA Project No. 85 (1975). Generally, the shear strength appears to have most importance in connection with adfreeze bonding. However, according to Frederking and Gold (1975) and Schwarz et el. (1974), the vertical tensile strength is of the greatest importance.

	Sea ice strength (MPa)	Comments	Reference
Tension	$\sigma_s = 2.80\ (1-\sqrt{\frac{V_b}{0.234}})$, $\sqrt{V_b} \leq 0.400$	Ring tensile tests	Frankenstein (1967)
	$\sigma_s \approx 0.66$, $\sqrt{V_b} > 0.400$		
	$\sigma_s = 0.82\ (1-\sqrt{\frac{V_b}{0.142}})$	Horizontal loading (Stress rate = 1-80 kPa/s)	Dykins (1967,1970)
	$\sigma_s = 1.54\ (1-\sqrt{\frac{V_b}{0.311}})$	Vertical loading (Stress rate = 1-180 kPa/s)	Dykins (1967,1970)
Compression	$\sigma_{sh} = 5.69\ (1-\sqrt{\frac{V}{0.188}})$	Horizontal loading (Strain rate = $10^{-3}s^{-1}$)	Vaudrey (1977)
	$\sigma_{sv} = 11.24\ (1-\sqrt{\frac{V}{0.424}})$	Vertical loading (Strain rate = $10^{-3}\ s^{-1}$)	Vaudrey (1977)
Bending	$\sigma_f = 7.35\times10^{-1}\ (1-\sqrt{\frac{V_b}{0.202}})$, $\sqrt{V_b} < 0.33$	Thin ice beams (h<40 cm)	Weeks and Assur (1967)
	$\sigma_f \approx 1.96\times10^{-1}$ $\sqrt{V_b} \geq 0.33$		
	$\sigma_f = 9.60\times10^{-1}\ (1-\sqrt{\frac{V_b}{0.250}})$	Small and large beams (h = 5 cm: Stress rate = 172-345 kPa/s; 170 cm $\leq h \leq$ 240 cm: Stress rate $\geq$ 96.5 kPa/s)	Vaudrey (1977)
Shear	$\sigma_f = 0.50-1.20$, $0.15 \leq \sqrt{V_b} \leq 0.35$	Small sample tests	Paige (1967)

Table I:2 Formulas for tensile, compressive, flexural (bending) and shear strength of sea ice.

3.7 Elasticity and Deformation Moduli

The elasticity modulus or Young's modulus Y and the deformation modulus or strain modulus E are often interchanged. However, as pointed out by Lavrov (1969) it is important to distinguish between these two moduli: a modulus is defined as the relationship between a stress and a strain or deformation. For ice, this relationship is calculated either by dynamic or by static measurements.

Young's modulus Y is defined as the ratio between stress σ and strain ε from dynamic tests (for example seismic measurements). In such tests the strain rate will be very high and the whole deformation may then be considered as purely elastic. Young's modulus depends only on the structure (porosity) of the ice.

The strain modulus E is defined as the ratio σ/ε from static tests and will therefore depend on both the ice structure and how the ice is being formed. The strain rate $\dot{\varepsilon}$ will usually be much lower than in dynamic tests, and the deformation may therefore contain both an elastic and a viscoplastic part ($\dot{\varepsilon} < 10^{-2}$ s^{-1}). It is found that the strain moduli calculated from tensile tests are higher than strain moduli calculated from compressive tests, while bending tests give values somewhere in between.

Very little information is available in the literature on the shear modulus of sea ice. However, the data examined shows, that the shear modulus is much less than the strain modulus.

It is found that Young's modulus Y is a linear function of V_b whereas the strain modulus E varies linearly with $\sqrt{V_b}$. For large brine volumes these characteristics are approximately constant.

Formulas for the above moduli are given in Table I:3.

	Strain modulus, E (GPa)	Stress rate kPa/s	Comments	Reference
Tension	4.03	23	Average of horizontal loading*)	Peyton (1966)
	7.05	23	Vertical loading*)	Peyton (1966)
Compression	0.78	53	Average of horizontal loading*)	Peyton (1966)
	1.70	53	Vertical loading*)	Peyton (1966)
Bending	$E_b = 5.32\ (1-\sqrt{\frac{V}{0.149}})$		Two-point loading	Vaudrey (1977)
Shear	G = 0.113	-	S=1.4o/oo, θ = -3.5°C	Lavrov (1969)
	G = 0.245	-	S=1.4o/oo, θ = -27°C	Lavrov (1969)
Young's modulus	$Y = 10\ (1-\frac{V_b}{0.285})$	Very high	Dynamic tests	Langleben and Pounder (1963)
Elastic shear modulus	$G = 3.86\ (1-\frac{V_b}{0.285})$	Very high	Dynamic tests and Pounder (1963)	Langleben

*) S = 0.18 - 3.6 o/oo

Table I:3 Formulas for the different moduli for sea ice.

4. Comparison between Polar Ice and the Ice in the Gulf of Bothnia

In order to be able to extrapolate the findings of the investigation of the Swedish offshore lighthouses to offshore installations in Arctic areas it is important to form an opinion of the differences and similarities in environmental impact.

When discussing differences in the impact of different types of sea ice on offshore structures in terms of interaction with construction materials the most important parameter is ice strength. From the above discussions it can be concluded that ice strength is primarily a function of grain size, salinity and temperature. The strength increases as grain size, salinity and temperature decrease.

When comparing polar ice and ice in the Gulf of Bothnia with respect to strength, salinity and temperature are the most important factors as grain size depends on factors other than geographic location, for example the meteorological and hydrodynamic conditions existing at the time of formation.

It can be concluded that multi-year polar ice presumably still has a higher salinity than ice in the Gulf of Bothnia, which is first-year ice as it does not survive the melting season, in spite of the reduction in salinity due to melt water drainage. However, owing to the lower temperatures that can be expected in the Arctic region, multi-year polar ice will probably have approximately the same strength as ice in the Gulf of Bothnia.

A comparison between multi-year polar pressure ridges and pressure ridges in the Gulf of Bothnia, however, speaks in favour of the polar ice. First-year ridges in the Gulf of Bothnia have a low salinity and are made up of individual pieces of ice which are poorly bonded. On the other hand, in a multi-year polar pressure ridge, the melt water produced during the summer months will drain downward into the core of the ridge. Then the water will refreeze, cementing the ice blocks together into a solid, resistant mass of low salinity. However, the salinity will probably not be as low as for ridges in the Gulf of Bothnia. A multi-year polar ridge can thus be expected to be stronger than a first-year ridge in the Gulf of Bothnia despite the somewhat

higher salinity. The influence of the lower temperatures in the Arctic will only serve to make the ice even stronger.

In conclusion, it can be stated that the ice in the Gulf of Bothnia is quite representative in comparison with the multi-year Arctic ice. However, consideration must be given to the differences especially as regards pressure ridges.

Nevertheless, a comparison between higher-salinity first-year polar ice and pressure ridges with the ice and pressure ridges in the Gulf of Bothnia would indicate the "Swedish" ice as being the strongest.

When discussing the impact of ice in terms of interaction with construction materials in absolute terms, i.e. not as a comparison between different types of ice, the following factors are also, of course, of predominant importance:

- Ice feature (level ice, rafted ice, pressure ridges, icebergs)
- Ice failure mode (ductile or brittle crushing, tension, bending, shear)
- Contact between ice and structure (contact area, degree of momentary contact, variation in contact)
- Structural shape (vertical or inclined face, shape or cross-section, width)
- Structural response (rigid, flexible, vibrating)
- Construction material properties.

APPENDIX II

DURABILITY OF CONCRETE IN MARINE ENVIRONMENT

1. Introduction

In the following, the durability of concrete in marine environments will be discussed in terms of resistance to different forms of environmental impact. The different impact modes discussed are chemical attack, freezing and thawing, corrosion of reinforcing steel and abrasion-erosion. The presentation is based on literature studies and is intended to be a general review of the state-of-the-art. Of specific interest for the present project is the resistance of concrete to the abrasive action of ice. However, no literature on ice abrasion has been available. Hence, the discussion on abrasion is in general terms.

2. Chemical Attack

2.1 Introduction

The most severe form of chemical attack by sea water on concrete is considered to be the attack by salts, and, among these especially sulphates. This is, however, not common in Swedish waters owing to the low salinity, see Table II:1.

Ion type	Ion concentration in kg/m³				
	Baltic Sea (average)	Bay of Kiel	North Sea (average)	Helgo-land	Atlantic Ocean (average)
SO_4^{2-}	0.58	1.25	2.22	2.78	2.81
Mg^{2+}	0.26	0.60	1.11	1.33	1.41
Ca^{2+}	0.05	0.19	0.43	0.43	0.48
Cl^-	3.96	8.96	16.85	19.89	20.00
Na^+	2.19	4.98	12.20	11.05	11.10
K^+	0.07	0.18	0.55	0.40	0.40

Table II:1 Ion concentration in different types of sea water in kg/m³ (Svensk Byggtjänst (1980)).

Other forms of chemical attack are aggregate reactions and salt crystallisation.

2.2 Sulphate Attack

The influence of different aggressive substances, incl. sulphates, in sea water and measures to meet attack are illustrated in Tables II:2-3.

The mechanism of deterioration is not completely clear, but the lime and the aluminates in the cement paste are obviously attacked during the formation of new solid substances, which, owing to their larger volumes often have a bursting effect.

At high sulphate concentrations, the free lime in the cement paste will most probably react with the sulphate ions during the formation of gypsum, which crystallizes in the concrete accompanied by an increase in volume of the solid phase of approx. 8%.

$$Ca(OH)_2 + SO_4^{2-} + 2H_2O \rightarrow CaSO_4 \times 2H_2O + 2OH^-$$

The mechanism at normal sulphate concentrations is less clear. In the past, it was generally believed that the hydration products of C_3A in the cement paste react with sulphates during the formation of a swelling compound called Ettringit or the "cement germ". The increase in volume of the solid phase during this reaction is due largely to the volume of the Ettringit.

$$3CaSO_4 + 4CaO \times Al_2O_3 \times 12H_2O \rightarrow 3CaO \times Al_2O_3 \times 3CaSO_4 \times 31H_2O + Ca(OH)_2$$

(Ettringit)

There are indications that a low percentage of free lime and a low pH value result in a non-swelling type of Ettringit. At the lime percentages and pH values in the case of the void water in standard Portland cement concrete, however, the swelling and destructive type of Ettringit will be formed.

According to a more recent hypothesis it is believed that there is another compound that is formed during swelling when the C_3A products react with the sulphate ions (Chatterji & Jeffery (1963)).

The sulphate content in sea water is high enough to give rise to severe sulphate attack. However, this does not usually take place owing to the

fact that the HCO_3- -ions in the sea water will react with free lime in the concrete, thus forming a protective layer of $CaCO_3$ (Locher (1968)). The bursting sulphate attack will thus not occur, but instead there will be a surface attack as the lime leaches, making the surface layer porous. The reason for this is probably the high content of magnesium ions in sea water.

Sulphate attack occurs on concrete manufactured from cement with a high C_3A content and having a high content of free calcium hydroxide. One way of decreasing the risk of sulphate attack is to use a cement with an increased sulphate resistance, i.e. a low C_3A content. ASTM has two limits for the C_3A content: 8% for Type II cement and 5% for Type V cement. $C_3A \leq 3\%$ is required for German and $C_3A \leq 3.5\%$ for English sulphate-resistant cement according to DIN 1164 (1978) and BS 4027 (1972), respectively. The Swedish cement of today generally has a C_3A content of 8-9%. However, Cementa AB has recently introduced a new low-alkali and sulphate-resistant cement with a C_3A content of $\leq 3\%$ thus fulfilling the requirements of ASTM, DIN and BS standards.

However, the C_3A content is not the only important parameter. Instead there is an interplay between the aggressive sulphate ions and the tightness of concrete which can be expressed through the water-cement ratio and the cement content, see Table II:3.

Another method of decreasing the risk of sulphate attack is to mix pozzolanes, for example silica fume and fly ash, into the cement. Pozzolanes consist of silica-rich powder with a large specific surface in the order of 500-20 000 m^2/kg. They react with the free lime during the formation of calcium hydro silicates possessing the same character as those created by the Portland cement. In this way the free calcium hydroxide is bonded thus preventing the formation of the swelling and destructive forms of Ettringit and gypsum.

Slag cement is very resistant to sulphate. According to Locher (1966), cement with more than 65% slag is always more sulphate resistant than the Portland cement included in the mix. The reason for this is partly that some of the aluminates in the slag are chemically bonded, i.e. inaccessible for chemical reaction, and partly that the content of free lime is considerably lower than in the pure Portland cement.

Both sulphate resistance and durability against other attacks increases with decreasing water-cement ratio. Consecuently the permeability of the concrete will be so low that ordinary cement is often sufficient. Fig. II:1 shows the relation between permeability and water-cement ratio.

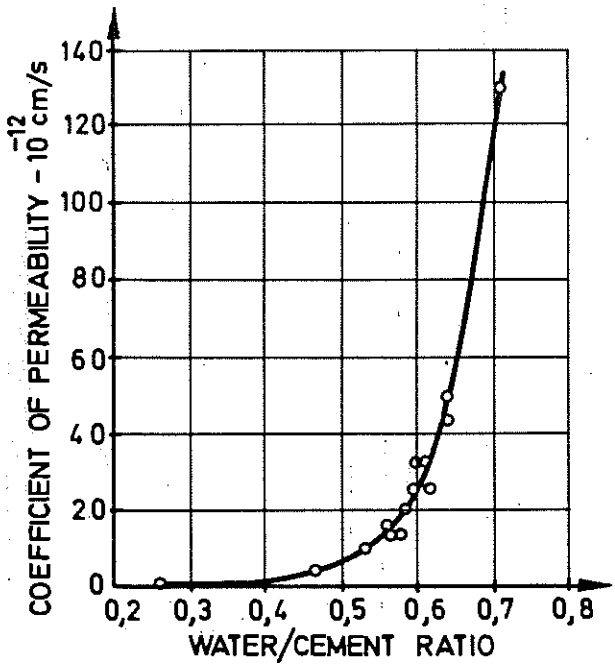

Fig. II:1 Relation between permeability and water-cement ratio in cement paste (Powers et al. (1954)).

Other measures that can be taken, possibly as a complement to a low water-cement ratio, are the use of greater concrete cover, special cement or protective coating. In addition, good compaction and careful curing are of course essential.

	Degree of Attack				
	None	Light	Moderate	Severe	Very Severe
pH	>6.5	6.5-5.5	5.5-4.5	4.5-4.0	<4.0
Aggressive CO_2 (mg CO_2/l)	<15	15-30	30-60	60-100	>100
Ammonium (mg NH_4^+/l)	<15	15-30	30-60	60-100	>100
Magnesium (mg Mg^{2+}/l)	<100	100-300	300-1500	1500-3000	>3000
Sulphate (mg SO_4^{2-}/l)	<200	200-600	600-3000	3000-6000	>6000

Table II:2 Assessment of the degree of chemical attack on concrete by water containing aggressive substances (Cembureau (1978)).

	Degree of Attack					
	None	Light		Moderate	Severe	Very Severe
Aggressive substances containing sulphates		Sulphate content Mg SO_4^{2-}/l water				
		200-400	400-600			
Cement type	OC	OC	OC	SRC	SRC	SRC	SRC
Max water-cement ratio	-	0.55	0.50	0.55	0.50	0.45	0.45
Min cement cont. (kg/m³)	-	300	330	300	330	370	370
Complementary protection of the concrete	-	-	-	-	-	-	Necessary
Aggressive substances not containing sulphates							
Cement type	OC		OC	OC	OC	OC	OC
Max water-cement ratio	-		0.55	0.50	0.45	0.45
Min cement cont. (kg/m³)	-		300	330	370	370
Complementary protection of the concrete	-		-	-	-	Necessary

Notes: OC = Ordinary cement
SRC = Sulphate-resistant cement, i.e. cement that is specified as being sulphate-resistant in accordance with the national standards.

Table II:3 Measures to meet chemical attack on concrete by water containing aggressive substances (Cembureau (1968)).

2.3 Aggregate Reactions

2.3.1 Introduction

Certain types of aggregates react under unfavourable conditions with the cement paste during the formation of swelling reaction products. This applies primarily to aggregates containing alkali soluble silica and silicates, certain types of magnesia limestone (dolomite), soluble sulphates or pyrites.

Thorough reviews of types of attack are given by Woods (1968) and Swenson (1972).

Damage due to aggregate reactions has so far been relatively rare in Sweden, primarily owing to a large supply of good quality aggregates. A possible change-over to lower quality aggregates and to cement with a higher alkali content may increase the risk of damage in the future.

2.3.2 Alkali-silica Reactions

Aggregates containing alkali soluble silica react with the alkalic void water solution during the formation of alkali-silica gel. In humid environments, water is absorbed during swelling thereby creating forces great enough to cause very extensive crack formation. In less severe cases only local pop-outs caused by isolated reactive aggregate particles close to the concrete surface will occur. In the case of alkali-silica damage, a viscous gel can often be seen being forced out in the cracks. The aggregate types of immediate interest have constituents such as opal, firestone calcedon, krypto crystalline quartz, ryolites and some volcanic species of stone, etc.

For severe swelling, a certain combination of reactive aggregates, particle size and access to alkali is required, either from the cement or from another source, and a high moisture content in the concrete. At low alkali contents no severe swelling will occur. According to ASTM, the alkali content of cement to be used together with reactive aggregates must be limited to 0.6%, calculated as an equivalent amount of natrium oxide, Na_2O, i.e. $Na_2O+0.658\ K_2O$.

Given sufficiently low or high contents of reactive aggregates, there will be no harmful expansion, irrespective of the amount of alkali. In the first case the content of reactive silica

will be too low whereas in the latter case the concentration of alkali will be too low, see Fig. II:2. The figure applies for a certain particle size. Different aggregate materials and particle sizes will give other graphs. It has been demonstrated that both very small and very large particles create small expansions.

Reviews of alkali-silica attacks are given by Nürnberg, Wolff, Hirche & Ludwig (1973-74), Diamond (1975-76) and Verein Deutscher Zementverke (1973). Guidelines for avoiding these problems are given in, for example, DIN Taschenbuch 37 (1979).

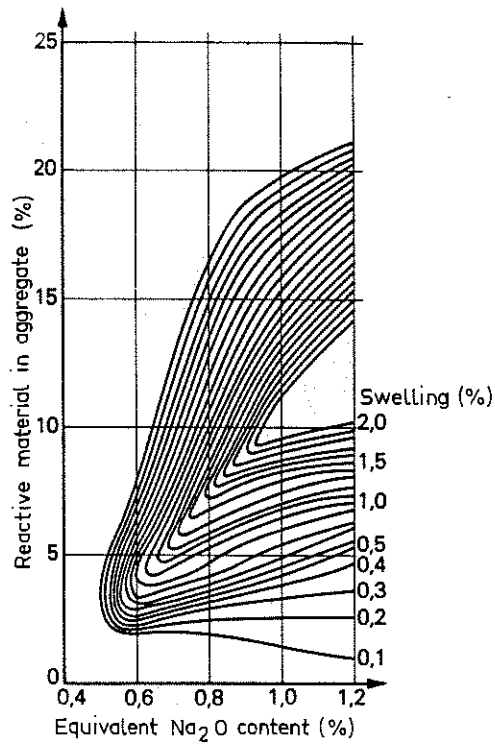

Fig. II:2 Example of swelling caused by alkali-silica reactions. Each curve corresponds to a certain constant swelling (Bredsdorff et al. (1962)).

2.3.3 Alkali-Carbonate Reactions

Certain carbonate species of stone, usually containing magnesia limestone (dolomite) and a clay component, can react with alkali hydroxide in the void water during the formation of expanding combinations. The swelling can be considerable and has caused great damage in, for example Canada and the USA. There are no known cases of this phenomenon in Sweden. Also the risk of this type of damage occurring will be reduced when using low-alkali cement, $\leq$0.4% equivalent Na_2O. For

further information, see Highway Research Board (1964) and Transportation Research Board (1974).

2.3.4 Sulphur Combinations

Aggregates sometimes contain sulphur combinations, usually in the form of sulphates and sulphides, which can cause expansion. Sulphate-containing material, usually containing gypsum or anhydrite, can be found in the Middle East and the USA. Also some artificial aggregates contain sulphates. The question of how much sulphate can be allowed in the aggregates is open to dispute. The West German standards DIN 4226 allow for up to 1% SO_3 in dried aggregates. British standards with some exceptions state that the total SO_3 content in the concrete mix must not exceed 4% of the cement content. Unsoluble sulphates such as barium sulphate are completely harmless. Pyrites, alum slate and other materials containing sulphide can cause a rare cement-aggregate reaction. The pyrites will be oxidized by the air during the formation of sulphates which react with the cement, probably accompanied by the formation of Ettringit. The form of attack is similar to sulphate attack, see Chapter 2.2. For further information, see Roosaar and Vessby (1962) and Hagerman & Roosaar (1955).

2.4 Salt Crystallization

A diffusion process always takes place proportional to the gradient of chemical activity. For intrusion of fresh water into concrete the diffusion is so slow that it can be neglected, while in the case of salt water, the driving gradient can be considerable if some of the pores contain water with a higher salt concentration than others. The conditions may be very complicated if the fluid or the dissolved components also enter into some chemical reaction with the components of the cement. Ideal solutions consisting of one gram molecule of a salt dissolved in one litre of water will give rise to an osmotic pressure of 22.4 atmospheres. For sodium chloride this means that 29 grams per litre of water, which is half the molecular weight of sodium chloride, can cause an osmotic pressure of this magnitude, i.e. that ordinary seawater can generate an osmotic pressure corresponding to a 300 metre water column (Rosenqvist (1959)).

If the salt concentration is increased by evaporation, considerable osmotic pressure gradients can develop. Pure water will thus try to diffuse

from the weaker salt solution towards the more concentrated solution, while at the same time there will be a flow of concentrated salt solution in the opposite direction. If both the diffusion and the flow are rapid compared to the evaporation from the surface, the osmotic processes will be able to efficiently reduce the transference of salt into the cement paste, and the transference of salt will be nearly equal in both directions.

If the salt water flowing upwards through the concrete should reach saturation point, salt crystals will form and continue to grow as evaporation proceeds. Such crystal growth will generate hydraulic pressure similar to that produced during formation of ice, compare Chapter 3.

3. Freezing and Thawing

3.1 Introduction

The deterioration of concrete exposed to freezing and thawing is caused by the expansion of freezing water in the void system of the cement paste or the concrete aggregates. However, the development of volume changes proves to be rather complicated as a number of variables are involved. The frost resistance of concrete depends on water absorption, air content and critical degree of saturation. The latter factor also includes other variables, such as distribution of air voids, strength of the paste, permeability and rate of freezing. The most significant theories regarding the mechanisms of freezing and thawing deterioration have been advanced by T.C. Powers and his associates.

3.2 Freezing in Capillaries and Generation of Hydraulic Pressure

Warris (1964) has shown that pastes with water-cement ratios of not lower than about 0.5, frozen at a moderate rate, have a critical degree of saturation of approx. 0.9, while in general this critical value is not lower than 0.6. When excess water in the larger cavities begins to freeze, the volume of water plus ice will exceed the original volume of the cavity. Therefore, as the water in the capillaries changes to ice, either the cavity must be dilated or the excess water be expelled from it.

Cement paste is a permeable material although the coefficient of permeability is extremely

low. Hence, there is a possibility of excess water escaping from a capillary during the process of freezing. If the diagram in Fig. II:3 is taken as representing half the material between two air voids, it can be seen that there is a possibility of excess water in the capillary escaping to the nearest air void. The growing ice body in the capillary will force the water through the paste toward the void boundary. Such a movement involves the generation of pressure. Factors affecting this pressure are:

- The coefficient of permeability of the material through which the water is forced.
- The distance from the capillary to the void boundary.
- The rate at which freezing occurs.

When water freezes in a capillary close to the escape boundary, the excess water can escape from this capillary more readily than from one further away. In general, during the process of freezing, hydraulic pressure will exist throughout the paste. This pressure will be higher at points further away from an escape boundary. If a point in the paste is sufficiently remote from an escape boundary, the pressure will be high enough to stress the surrounding gel above its tensile strength, and hence produce permanent damage.

All air voids in cement paste are assumed to have a border zone in which the hydraulic pressure cannot become high enough to cause damage. Theoretically, the pressure increases approximately in proportion to the square of the distance from the void, the pressure being zero at the void boundary. By reducing the distance between voids to the point where the protected zones overlap, generation of disruptive hydraulic pressu-res during the freezing of water in the capillaries can be prevented.

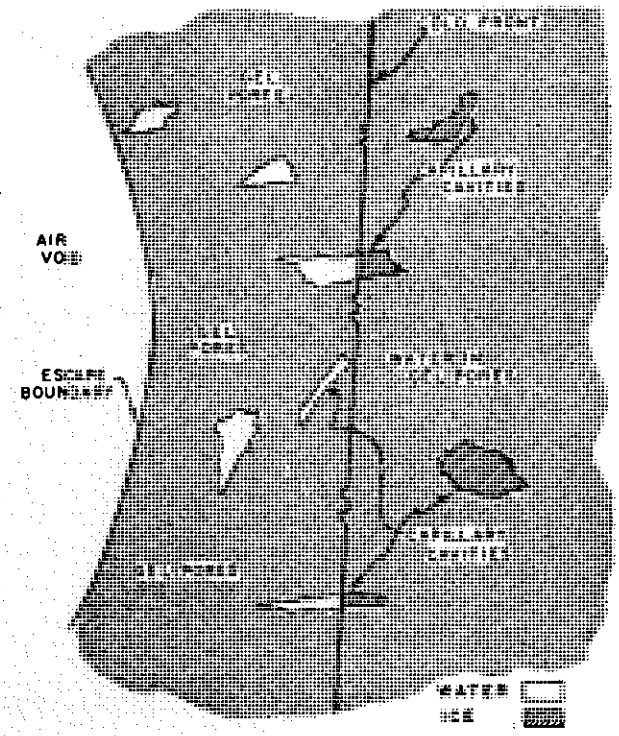

Fig. II:3 Diagram of the pore structure of Portland cement paste, based on studies by Powers. If the air void (left) were to be of average size and drawn to scale, curvature would hardly be discernible in a diagram of this size (Cordon (1966)).

Experimental data by Powers and Helmuth (1953) have verified this hypothesis. Fig. II:4 shows that shrinkage takes place before cooling has advanced to the point where the water first starts freezing, and as freezing continues, rapid expansion takes place. Considering a capillary cavity, hydraulic pressure will first appear in this cavity at the instant when freezing begins. The magnitude of the pressure will depend on the rate of freezing and the ease with which water is forced from the cavity. Therefore, the paste as a whole, acted on simultaneously by all similar cavities, should start to expand at the instant freezing begins, as indicated by Figs II:4-5. No other mechanism presented to date can account for this coincidence of events. However, generation of hydraulic pressure does not account for all the phenomena caused by freezing of cement paste. Furthermore the conditions in the capillaries after ice has formed must be considered.

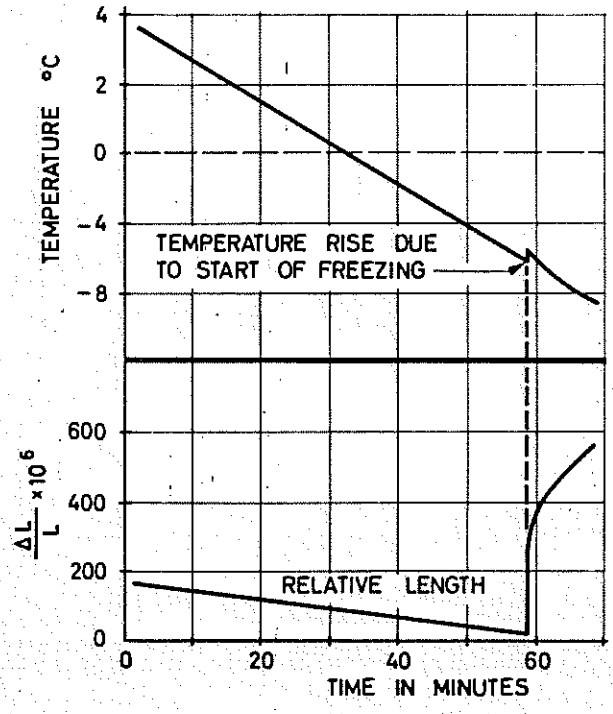

Fig. II:4 Coincidence of initial expansion at the start of freezing (Powers and Helmuth (1953)).

3.3 Diffusion and Freezing of Gel Water in Capillaries

The ice in the capillaries of frozen cement paste is surrounded by unfrozen water in the gel pores. If the gel is saturated, the gel water has the same free energy as that of ordinary water in bulk. There is thermodynamic equilibrium between the gel water and the ice in the capillary at 0°C, assuming that both the ice and the gel water are under a pressure of one atmosphere, and the capillary is so large that surface energy is negligible. If the temperature drops below the freezing temperature of the water in the capillary, the gel water is no longer in thermodynamic equilibrium with the ice; its free energy is higher than that of ice. The gel water thus acquires an energy potential enabling it to move into the capillary cavity, where it freezes and causes the ice crystals to grow.

The gel has a tendency to shrink as water is diffused. On the other hand, the growth of the ice body in the capillary puts the ice and the film around it under pressure.

The swelling pressure in the ice film is high enough to produce expansion of the paste. For example, if the gel pores were saturated and the capillary cavities contained ice at -5°C, pressure in the film between the ice and the solid gel can be as high as 85 kp/cm^2. This pressure would cause the paste to dilate appreciably and the concrete to expand. This explains why continued expansion occurs in non-air-entrained paste after freezing water in the capillary cavities has expelled the excess water. See Fig II:5.

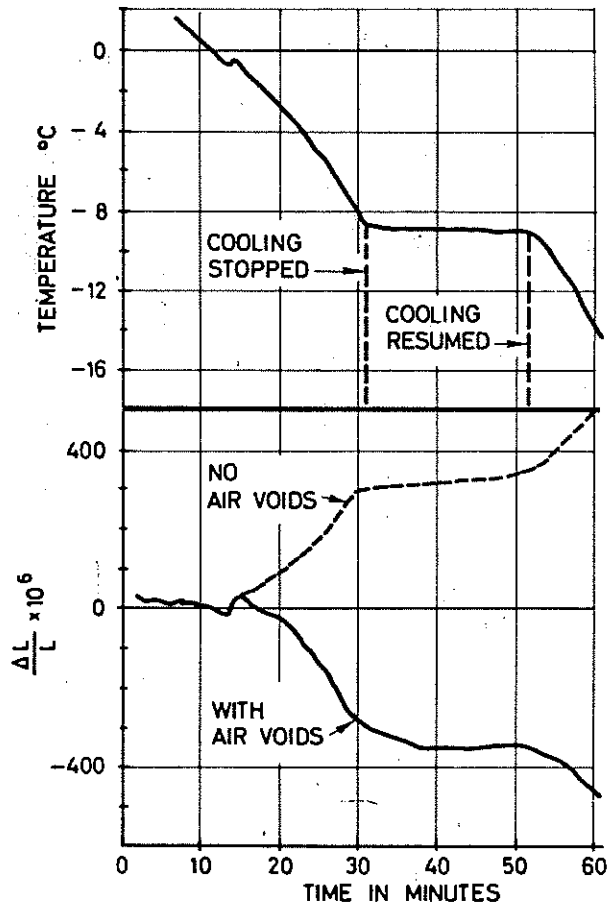

Fig. II:5 Dimensional changes in cement paste with and without air voids (Powers and Helmuth (1953)).

The question arises of whether or not entrained air voids protect the concrete from receiving ice pressures built up in the capillary voids. From the considerations of thermodynamics it can be seen that gel water will not only diffuse to the capillary cavites, but will also diffuse

to ice previously forced into the air voids by hydraulic pressure.

The volume of the ice in the air void is not usually equal to the volume of the void. Consequently, the volume expansion of this either results in no expansive force at all or at most a very small one. The net effect of water lost from the gel to the air void is a tendency towards shrinkage. The amount of gel water that could enter capillary cavities by diffusion would be a maximum if the paste contained no air voids, and if the boundaries of the paste were at infinite distance from the cavity. In this case, the capillary ice would grow as long as neccessary to reach equilibrium with the gel water. If the stress, whether from hydraulic pressure or from subsequent growth of capillary ice, ruptured the gel and thus released the pressure of the ice, the growth would be limited only by the amount of freezable water in the system. On the other hand, if the paste contains air voids, the period of diffusion to the capillary cavities will be correspondingly short. Laboratory tests verify this assumption regarding the diffusion of gel water and the expansion of specimens efter freezing (Powers and Helmuth (1953)). As already mentioned, rapid expansion with freezing shown in Figs II:4-5 seems to be explainable only in terms of the hydraulic pressure generated during the freezing of capillary water. In Fig. II:5 the first and last part of the dashed-line curve represent expansion due to hydraulic pressure, while the slight expansion in between is due to diffusion of gel water to the capillaries. The bottom curve shows the behaviour of a similar specimen containing air voids.

It should be mentioned that an outside source of moisture which through cracks or fractures may replace the gel water during a thawing cycle, will theoretically provide moisture for unlimited growth of the ice crystals.

3.4 Mechanisms of Control

By using concrete with a low water-cement ratio, sufficient air content and frost-resistant aggregates in combination with good workmanship as regards casting and curing it is possible to obtain a very high degree of frost resistance even in very aggressive environments.

The relationship between frost resistance and water-cement ratio is illustrated in Fig. II:6.

The water-cement ratio must be kept below 0.5-0.6 in order to give sufficient frost resistance.

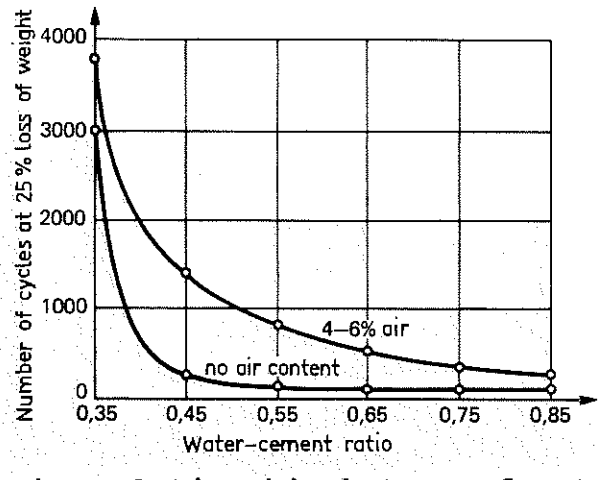

Fig. II:6 The relationship between frost resistance and water-cement ratio. (U.S. Bureau of Reclamation (1955))

Wide practical experience shows very clearly the positive effect of air content on the frost resistance of concrete. Fig. II:7 shows the results of tests carried out in fresh water on a large number of concrete mixes with varying compositions. The variation in results is relatively extensive as a consequence of variations in water-cement ratio and in the distribution of the air voids.

As regards the distribution of the air voids, it is more favourable if the voids, at the same air content, are many and small instead of fewer and larger, i.e. the spacing between the air voids shall be kept to a minimum.

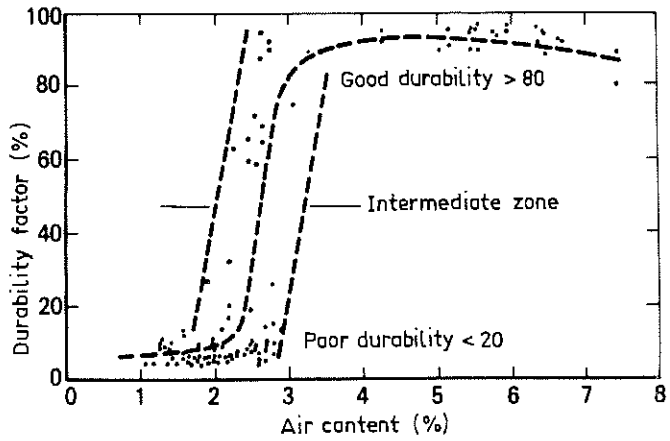

Fig. II:7 The influence of air content on the frost resistance of concrete in fresh water (Cordon (1966)).

If freezing takes place in sea water, there must be a combination of increased air content and a water-cement ratio below approx. 0.45. Increased air content alone is not sufficient.

4. Corrosion of Reinforcing Steel

4.1 Introduction

Embedded steel is protected against corrosion owing to the high pH value of the concrete.

Concrete normally has a pH value within a range of 12.5 to 13.2, and according to Shalon and Raphael (1959) the basicity of concrete should not drop lower than to a pH value of about 11.5 if it is to provide embedded steel with an adequate degree of protection.

Differences in the various types of cement are a result of variations in its composition, and therefore not all types of cement have the same ability to protect embedded steel. According to Pressler et al. (1961) a well-hydrated Portland cement may have a content of calcium hydroxide varying from about 15 to 30 per cent by weight of the original cement. This is sufficient to maintain a continuously saturated solution of calcium hydroxide in the concrete independent of moisture content. However, in contrast to straight Portland cements most types of cement, such as High Alumina cements, Portland Blast-Furnace cements and Portland-Pozzolana cements, will all have various amount of calcium hydroxide bound to reactive siliceous materials. Hence the reserve basicity of such cements is also lower.

Rosenqvist (1961) has described an example of exceedingly rapid steel corrosion in a tropical concrete wharf, where pozzolanic material was added to the Portland cement. Corrosion of the reinforcement appeared shortly after the construction was completed. From measurements of the pH value in extract from the concrete, no values above 11.5 were found, while the pH value of the concrete adjacent to the steel showed values of 5.7 to 8.5. When the pozzolana was omitted, an increase in the pH value was obtained, and no further damage was observed.

When the steel in concrete starts corroding, an accumulation of corrosion products will tend locally to reduce the basicity at the anode. As diffusion of corrosion products is slowed

down and hindered by the cement paste, a relatively rapid decrease in the pH value may occur, resulting in an even higher rate of corrosion.

Normally, a protective film is maintained on embedded steel because of the high pH value in the concrete. Nevertheless, even for cements with the highest reserve basicity, certain effects can impair the steel passivity, as discussed in the following.

4.2 Effect of Carbon Dioxide

A reaction between the atmospheric carbon dioxide and the calcium hydroxide solution in concrete will neutralize the basicity and form calcium carbonate with pH values below 8.5. Hence, a carbonation of concrete will impair the passivity of embedded steel.

In Germany, extensive investigations have been carried out on the carbonation depth in old concrete (Deutscher Ausschuss für Stahlbetong, H. 170 (1965)). With the exception of one case of particularly old concrete, in which carbonation depths of up to 85 mm were registered, none of the other concrete samples of varying types and ages up to 55 years old, showed depths of more than 25 mm. On the whole, the study confirmed the popular opinion that the action of carbon dioxide on good quality concrete is normally limited to a thin surface layer. However, carbon dioxide can penetrate further into porous concrete or cracks and in this way influence the basicity along the reinforcement.

Even if the concrete has carbonized all the way to the reinforcement, corrosion will not occur if the relative humidity of the concrete is less than 75-80%. In completely saturated concrete the rate of corrosion will then only reach the reinforcement slowly. The maximum rate of corrosion is at a relative humidity of approx. 95%. Also the temperature influences the rate of corrosion. An increase in temperature from 0°C to 30°C results in an increase in corrosion rate by factor 10.

4.3 Effect of Chlorides

The corrosion of embedded reinforcement can take place also in non-carbanized concrete. It is a well known phenomenon that even very small concentrations of chloride ions are capable of breaking the passivating oxide film on metals.

Bäumel and Engell (1959) have shown that if a saturated calcium hydroxide solution substitutes the concrete, concentrations even smaller than 0.0035 % of chloride ions have some effect on the passivity of steel. This highly important effect of chlorides is considered to be the main cause of all steel corrosion occurring in marine concrete structures.

Because small amounts of chloride ions frequently tend to form very small anodes and large cathodes, intensified corrosion and sharp pits over very small areas are produced. Pitting is a highly dangerous form of attack, as the resulting damage is so much out of proportion to the actual amount of metal loss.

Portland cements will normally react chemically with chlorides in solution, and thus have some ability to reduce the chloride concentration. Hence, the corrosive influence of chlorides in concrete is somewhat dependent on whether the chloride is introduced during or after the cement hydration. The degree of removal of chloride from the solution depends on the amount of calcium aluminate in the cement. This effect is discussed by Steinour (1964).

4.4 Mechanism of Control

The rate of carbonation decreases with decreasing permeability of the concrete, and thus with lower water-cement ratios. This is illustrated in Fig. II:8. See also Fig. II:1.

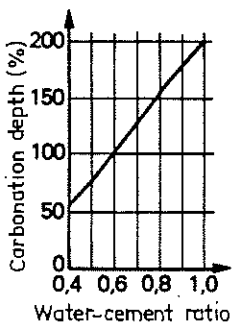

Fig. II:8 The relationship between carbonation depth and water-cement ratio (Meyer, Wierig & Hausmann (1967)).

Also the effect of chlorides decreases with lower water-cement ratios as can be seen from Fig. II:9.

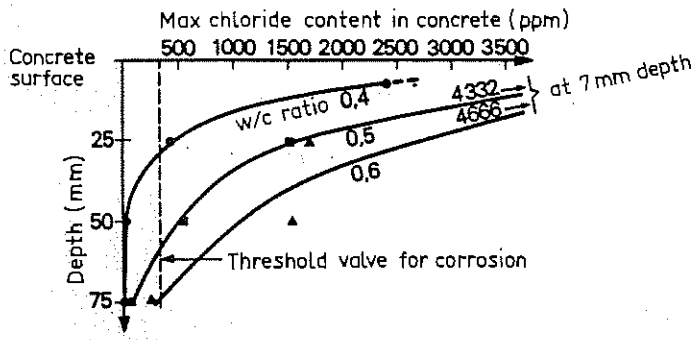

Fig. II:9 Chloride concentration in concrete slabs that have been sprayed with a 3 % NaCl solution for 330 days (Clear (1974)).

Clear (1974) says that the threshold value for corrosion due to chlorides is a chloride concentration of approx. 300 ppm. From Fig. II:9 it can, for example, be seen that the threshold value of 300 ppm will have been reached after 300 days at a depth in the concrete of 30 mm if the water- cement ratio is 0.4.

Another protective measure as regards reinforcing-steel corrosion is, of course, to increase the concrete cover.

5. Abrasion-erosion

5.1 Introduction

The literature on abrasion-erosion that is quoted in the following is mainly limited to the abrasion of horizontal surfaces. However, when discussing the impact of ice on offshore concrete structures, the abrasive action will, however, be related to vertical surfaces.

Degradation of a concrete surface due to abrasion can come about in different ways. On the one hand there may be a grinding effect against the surface. On the other there may be a tear-off of protruding particles in the surface, see Fig. II:10. The aggregate particles can be regarded as cantilevers restrained in the concrete surface and subjected to horizontal forces. In addition, pure crushing or splitting in the surface layer is possible if isolated, protruding particles are subject to large, concentrated loads.

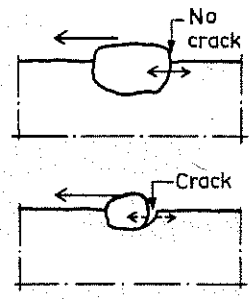

Fig. II:10 Tensile stresses arises in the phase boundary between cement paste and aggregates by horizontal forces. Smaller aggregate particles are more easily torn off than larger, more anchored ones (Paulsson & Samuelsson (1968)).

Abrasion resistance does not denote any absolute resistance or strength property, but instead means the ability of concrete to withstand abrasive action. In that respect compressive strength, tensile strength, etc. are important characteristics, either individually or in combination.

5.2 Factors influencing Abrasion Resistance

The factors that influence abrasion resistance are primarily:

- Concrete strength and composition
- Aggregate strength
- Workmanship
- Curing
- Surface conditioning

The influence of concrete strength is illustrated in Table II:4 and Fig. II:11.

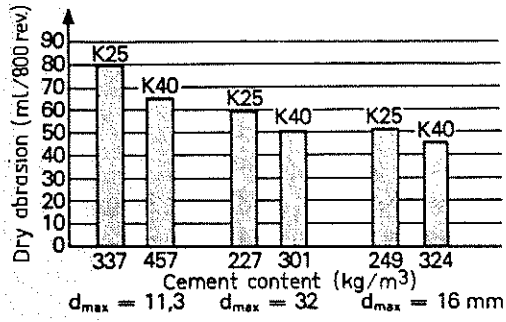

Fig. II:11 The influence of strength class (cement content) and max stone size, d_{max}, on abrasion. Dry abrasion according to the Bauschinger method (Paulsson & Samuelsson (1968)).

	Wet abrasion (ml)	Dry abrasion (ml)
Hard concrete containing carborundum and corundum	5-10	approx. 5
Hard concrete containing quartz	15-20	approx. 15
Vacuum concrete, d_{max} = 16 or 32 mm	15-25	approx. 15
Concrete K40, d_{max} = 16 or 32 mm	20-25	10-15
Concrete K25, d_{max} = 16 or 32 mm	20-30	15-20
Concrete K25, d_{max} = 8 mm (cement mortar)	30-40	20-30

Note: Concrete K40 = Concrete strength 40 MPa.

Table II:4 Results from abrasion tests according to the Bauschinger method. Abrasion in ml/200 revolutions in the interval of 400-800 revolutions. Wet abrasion according to Forsblad (1972) and dry abrasion according to Paulsson (1969).

An increase in compressive strength reduces abrasion to a certain extent, whereas a change-over from cement mortar to concrete with 16 or 32 mm max stone size considerably increases the abrasion resistance. Ottoson & Sahlman (1975) show that an increase in concrete strength reduces abrasion. No influence of max stone size, 4 mm, 16 mm or 32 mm, was observed. This contradicts the results in Fig. II:11 to a certain extent. One explanation may be different concrete mixes and different aggregate hardness in the two tests.

According to Springenschmid & Sommer (1971), the aggregate properties affect abrasion resistance. They have found that coarse aggregate particles make a considerable contribution to an increase in abrasion resistance. They also point out the importance of a cement paste with high strength in order to give the aggregate particles good anchorage.

One way of obtaining a stronger cement paste may be to add silica fume. Impregnation with polymers may be another solution.

Holland (1983) reports on an abrasion testing program carried out at the U.S Army Corps Engineers Waterways Experiment Station in connection with the Kinzua Dam Stilling Basin Rehabilitation Project in the USA. The program comprised both "conventional" and silica fume concretes. The results of some of the testing are shown in Fig. II:12.

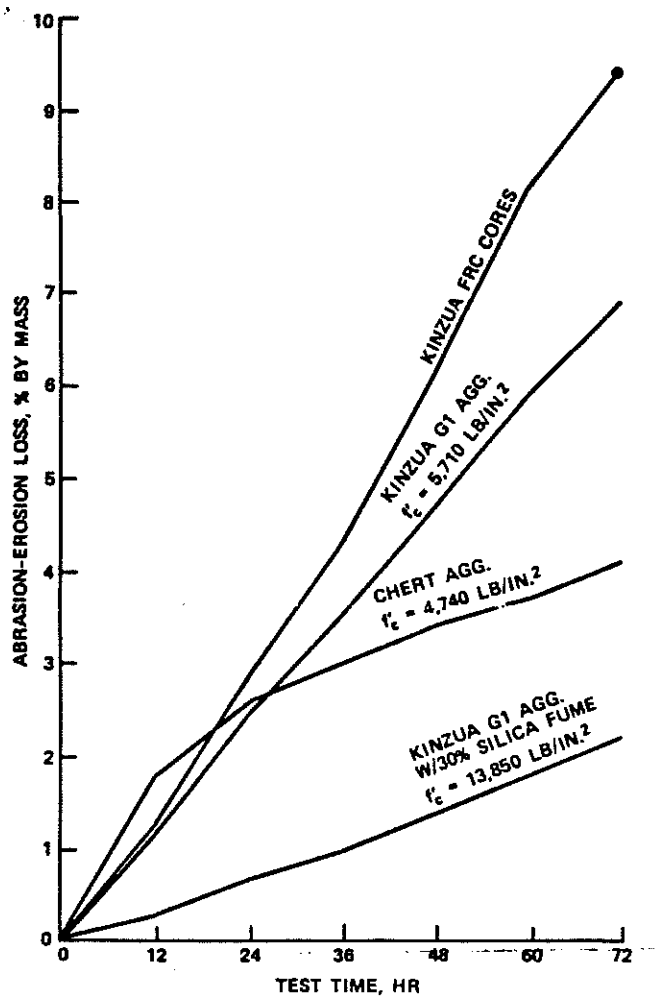

Fig. II.12 Results of abrasion testing accomplished for the Kinzua Dam Stilling Basin Rehabilitation Project (Holland (1983)).

The line labeled "Chert Agg." represents abrasion resistance of a very hard natural aggregate locally available at the testing station. The line labeled "Kinzua G1 Agg." represents a limestone aggregate locally available at the project site. The abration resistance was significantly improved when this latter aggregate was used in a silica fume concrete (bottommost line). The uppermost line in Fig. II:12 shows the abrasion loss of cores taken from the fiber-reinforced overlay that was placed in the Kinzua Basin in 1973 and 1974. The test method used for the above-mentioned testing has been standardized in the Handbook for Concrete and Cement as CRD-C 63-80, and is currently (Aug. 1983) being evaluated for acceptance by ASTM as a standard test method.

The surface layer is normally weaker than underlying concrete and if it is removed the abrasion will often be radically reduced. According to Springenschmid & Sommer (1971), the abrasion rate will be reduced to 1/10-1/20 when the fine-granular surface layer has been worn down and the aggregates uncovered. Harder aggregate types, such as (granular) corundum, Al_2O_3, and carborundun, SiC, increase abrasion resistance, see Table II:4.

The concrete shall be of such a composition that the least possible water and mortar separation arises on the concrete surface and the casting be carried out in a way that unnecessary water and cement mud are avoided on the surface. Vacuum concrete is one way of reaching this goal.

Abrasion tests carried out according to the Bauschinger method clearly show the difference in abrasion resistance between vacuum concrete and "normal" concrete, see Fig. II:13.

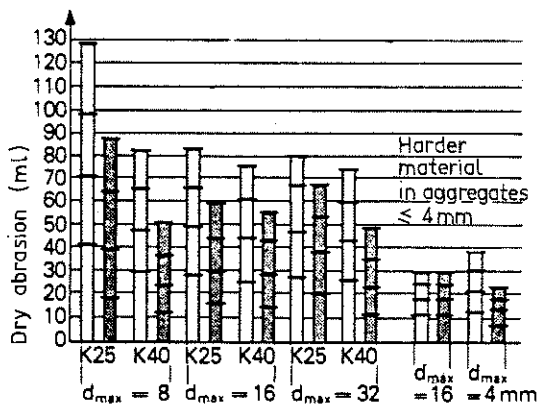

Fig. II:13 Comparison between abrasion of vacuum concrete (grey) and "normal" concrete. Dry abrasion according to the Bauschinger method. The cross lines mark 200 revolutions (Paulsson (1969)).

During the first 200 revolutions the abrasion for "normal" concrete was considerably greater than during the subsequent ones. This is due to the "mud" surface layer. This was not observed for the vacuum concrete.

According to Kennedy & Prior (1955), good curing by sparying water on the structure or preventing moisture wastage are important measures in order to obtain good abrasion resistance. Moist curing for 14 days instead of 3 days may result in twice as great an abrasion resistance.

Another way of increasing abrasion resistance is some sort of surface conditioning. One way of doing this may be to apply a surface coating, e.g. dense epoxy.

OG 306d-003d
JEJ/MIA/GA
1984-08-29